Naval Research Laboratory
Washington, DC 20375-5320

NRL/MR/6386--93-7369

Progress in the Modeling of the Shock Response and Mitigation of Thick Composite Shells

C. T. DYKA

Geo-Centers, Inc.
Fort Washington, MD

P. W. RANDLES

Mechanics of Materials Branch
Materials Science and Technology Division

July 22, 1993

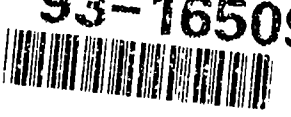

REPORT DOCUMENTATION PAGE

Form Approved
OMB No. 0704-0188

1. AGENCY USE ONLY (*Leave Blank*)	2. REPORT DATE	3. REPORT TYPE AND DATES COVERED
	July 22, 1993	

4. TITLE AND SUBTITLE

Progress in the Modeling of the Shock Response and Mitigation of Thick Composite Shells

5. FUNDING NUMBERS

6. AUTHOR(S)

C.T. Dyka* and P.W. Randles**

7. PERFORMING ORGANIZATION NAME(S) AND ADDRESS(ES)

Geo-Centers, Inc.
10903 Indian Head Highway
Fort Washington, MD 20744

Naval Research Laboratory
Washington, DC 20375-5320

8. PERFORMING ORGANIZATION REPORT NUMBER

NRL/MR/6386--93-7369

9. SPONSORING/MONITORING AGENCY NAME(S) AND ADDRESS(ES)

ARPA
Arlington, VA 22209

10. SPONSORING/MONITORING AGENCY REPORT NUMBER

11. SUPPLEMENTARY NOTES

*Geo-Centers, Inc.
**Presently at Defense Nuclear Agency, Kirtland AFB, NM

12a. DISTRIBUTION/AVAILABILITY STATEMENT

Approved for public release; distribution unlimited.

12b. DISTRIBUTION CODE

13. ABSTRACT (*Maximum 200 words*)

This report is a continuation of our efforts to develop a methodology for predicting the response of thick composite materials subjected to multi-dimensional shock loadings. A focus of this work has been the initiation and evolution of damage in 1D, 2D and 3D composite structures. In addition, dispersion/viscoelastic models have been investigated for 1D structures and implemented. One dimensional damage predictions are made for composite plates subjected to underwater shock. The 1D and 2D continuum damage models are both applied to the impact of a plexiglass flyer and graphite/peek plate, and the results compare very well to experimental data.

A new 3D continuum damage theory is developed for thick laminated composite plates. The 3D theory is in part an extension of the 2D transversely isotropic damage theory. However, three dimensional considerations as well as the inefficiencies of modeling individual plies in a thick composite require a slightly different approach. A 3D formulation is developed which applies the damage directly to the stresses, rather than the compliances as in the 2D and 1D theories.

14. SUBJECT TERMS

Composites	Finite difference	Plates and shells	Wave Propagation
Damage mechanics	Finite Element	Shock	UNDEX
Explicit analysis	Impact	Transient	

15. NUMBER OF PAGES

58

16. PRICE CODE

17. SECURITY CLASSIFICATION OF REPORT	18. SECURITY CLASSIFICATION OF THIS PAGE	19. SECURITY CLASSIFICATION OF ABSTRACT	20. LIMITATION OF ABSTRACT
UNCLASSIFIED	UNCLASSIFIED	UNCLASSIFIED	UL

CONTENTS

PROGRESS IN THE MODELING OF THE SHOCK RESPONSE AND MITIGATON OF THICK COMPOSITE SHELLS

1. INTRODUCTION

Future naval vessals are expected to utilize increasing amounts of thick polymer matrix composite materials in their structure due to significant system performance enhancements achievable with these stiff, strong, lightweight materials. In order to apply these materials to submarine and surface ship structures, their behavior under highly transient shock loadings must be better understood. Current analysis methods for impact and underwater shock response were developed primarily to predict the behavior of ductile, homogeneous metal structures, which under severe loads deform plastically due to slip along shear planes. Composites are very heterogeneous materials, combining high performance fibers in a viscoelastic matrix. Also, composites tend to be highly dispersive to propagating waves and deform nonlinearly under severe load through the development of networks of micro-cracks.

This report is a continuation of our efforts [1-5] to develop a methodology for predicting the response of thick composite materials subjected to multi-dimensional shock loadings. In developing the numerical aspects of this work, the explicit transient finite element programs PRONTO2D [8] and ABAQUS/EXPLICIT[9] are being employed to construct two dimensional (2D) and three dimensional (3D) capabilities. In addition, the explicit finite difference program WONDY[7] is being used to study one dimensional (1D) behavior and to develop advanced material models relating to evolving damage, dispersion and viscoelasticity. Appendix A contains a brief description of the reduced 1D damage model with nonlinear compression, which has been programmed into WONDY. This constitutive model is based upon the 2D continuum damage model developed in [1-3].

In section 2, the inclusion of dispersion effects in the 1D damage in the damage model is discussed. The use of higher derivatives in the constitutive modeling is explored as well as predictions for composite plates subjected to underwater shock. The effects of viscoelasticity in the matrix of the composite plate and its effect on dispersion is also addressed.

The application of the 2D continuum damage theory is discussed in section 3. A comparison is made with PRONTO2D models to 1D damage results from WONDY predictions for the impact

Manuscript approved May 19, 1993.

of a plexiglass flyer and graphite/peek plate - see [6] for the experimental results. This is followed by a coarse model of 2D impact using the PRONTO2D program.

In section 4, a 3D continuum damage theory is developed for thick laminated composites. The 3D formulation in part is an extension of the 2D transversely isotropic damage theory [1-3]. However, three dimensional considerations as well as the inefficiencies of trying to model individual plies in a thick composite require a slightly different approach. In this section, a 3D formulation is developed which applies the damage directly to the stresses as in [10-12], rather than the compliances as is the case in the 2D theory.

ABAQUS/EXPLICIT [9] will in the future be the major developmental code for 2D and 3D finite element analysis replacing PRONTO. Appendix B is a listing of the ABAQUS/EXPLICIT user written subroutine for 2D continuum damage, and is similar to the 2D damage model programmed into PRONTO2D.

Finally in sections 5 and 6, a summary is given followed by some thoughts on future directions.

2. DISPERSION EFFECTS IN A 1D DAMAGE MODEL

2.1 Background and general remarks

Composite materials, especially laminated plates and shells, comprise a very heterogeneous media. The dynamic response of such materials can be broadly classified into one of two groupings [13]. If the wavelength of the loading and the response of the material is very long compared with the scale of the inhomogeneity, then the material response is governed by effective properties of the equivalent homogenized media. However, if the composite structure is subjected to shock loadings such as UNDEX or impact, then the wavelengths of the loading and the response of the structure are much shorter. If this is the case, the characteristic dimensions of the hetergeneous media become much more important and the dynamics is greatly complicated. The interfaces between the material phases cause wave reflection and refraction. The energy is thus spread or "dispersed" over many wavelengths. Mathematically this implies that the phase speed c and the frequency ω are a function of the wavelength k [13-14] or:

$$c(\omega) = \frac{\omega(k)}{k} \qquad (2.1a)$$

In a non-dispersive media, the phase speed equals the wave speed and is a constant. The frequency is then expressed as:

$$\omega = c_0 \cdot k \qquad (2.2b)$$

Dispersion in composite materials can have two sources. We have already discussed the role that geometry changes can play in a heterogeneous media. Another form of this phenomenia has as its origins the viscoelastic nature of the matrix of the composite. Separating the geometric and the viscoelastic effects is, however, a very difficult undertaking. In [15] Sutherland discusses this very problem.

For our purposes, however, it is not necessary in the numerical methods to completely separate these two sources of dispersion. Rather what is needed is an approach that can accurately take into account dispersion in general without requiring an excessive number of degrees of freedom and associated computer costs.

Before describing the specific details of our approach, we note that as discussed in [14], the phenomenon of dispersion can be introduced directly into the numerical schemes such as finite differences and finite element methods. For homogeneous media, numerical dispersion is not desired since it represents additional error and inaccuracy in the response of the system being modeled. However as indicated in [14,16-17], unwanted numerical dispersion is usually present in computer models.

2.2 Development of an approach and application

For a heterogeneous media, the problem encountered involves the inclusion of the dispersive effects without the need to explicitly model all the fine details of the materials, which would require a very large number of degrees of freedom. One approach is to introduce higher derivatives into the governing equations [17-18]. In [17], longitudinal waves in a plate are studied. The classical wave equation is:

$$\frac{\partial^2 u}{\partial t^2} = c_0^2 \frac{\partial^2 u}{\partial t^2} \tag{2.2}$$

where u is the longitudinal displacement and c_0 is the wave speed (non-dispersive). To include dispersion effects, a fourth order partial differential equation is substituted in place of (2.2) that has the form:

$$(\frac{\partial^2}{\partial t^2} - \alpha^2 \frac{\partial^2}{\partial x^2})\, u + \kappa\,(\beta^2 k^2 - \omega^2)\,(\gamma^2 k^2 - \omega^2) = 0 \tag{2.3}$$

where α, β, γ and κ are constants chosen to satisfy the governing dispersion equation.

An approach similar to [17] has been incorporated into the one dimensional program WONDY in an attempt to include dispersion effects due to the heterogeneity of the composite material [4,19]. For a 1D case, the stress strain relationship can be written as:

$$\sigma = C_{11}\varepsilon \tag{2.4}$$

Next higher derivatives with respect to time are introduced into eq. (2.4) in the form:

$$\frac{\partial^2}{\partial t^2}(\sigma - C_{11}\varepsilon) + \frac{2}{\lambda_1}\frac{\partial}{\partial t}(\sigma - \gamma_1 C_{11}\varepsilon) + \left(\frac{1}{\lambda_1^2} + \frac{1}{\lambda_2^2}\right)(\sigma_1 - \gamma_2 C_{11}\varepsilon) = 0 \tag{2.5}$$

where λ_1, λ_2, γ_1 and γ_2 are empirical constants to be determined by matching with experimental results. Equation (2.5) is a relatively straight forward constitutive relation and its numerical integration within an explicit program such as WONDY would appear to be routine. In fact, the integration using Runge-Kutta methods of eq. (2.5) proved to be quite challenging, requiring even finer time steps than needed by the central difference operator used in WONDY to integrate the equations of equilibrium. The use of explicit numerical integration for the constitutive relation eq. (2.5) thus proved to be too expensive.

Another approach to the integration of eq. (2.5) is to express it in a convolution product form such as:

$$\sigma = (G \otimes \dot{\varepsilon}) \tag{2.6}$$

where $\otimes$ represents the convolution. Toward this end, one can take the Laplace transform of eq. (2.5) assuming zero initial conditions [19]. Doing this and then performing an inverse Laplace transformation produces:

$$\sigma(t) = H(t) \int_0^t G(t-t') \dot{\varepsilon}(t')\, dt' \tag{2.7}$$

where $H(t)$ is the Heaviside function, and $G(t-t')$ is a function of t, t', γ_1, γ_2, λ_1 and λ_2 - see [19]. Equation (2.7) has the general form of the hereditary integrals produced in viscoelasticity theory [20]. The stress at time t_{n+1} can be expressed by:

$$\begin{aligned}\sigma(t_{n+1}) = \gamma_2 \varepsilon(t_{n+1}) + e^{-t_{n+1}/\lambda_1} &\left(\frac{\lambda_2}{\lambda_1} (2\gamma_1 - \gamma_2 - 1) \sin\left(\frac{t_{n+1}}{\lambda_2}\right) \quad (1-\gamma) \cos\left(\frac{t_{n+1}}{\lambda_2}\right) \right) \\ &\times \sum_{j=1}^{n+1} e^{\frac{t_j}{\lambda_1}} I_c^j \quad - \\ e^{-t_{n+1}/\lambda_1} &\left(\frac{\lambda_2}{\lambda_1} (2\gamma_1 - \gamma_2 - 1) \cos\left(\frac{t_{n+1}}{\lambda}\right) \quad (1-\gamma_2) \sin\left(\frac{\lambda_{n+1}}{\lambda_2}\right) \right) \\ &\times \sum_{j=1}^{n+1} e^{\frac{t_j}{\lambda_1}} I_s^j \end{aligned} \tag{2.8}$$

where

$$I_c^{j+1} = E\dot{\varepsilon}^{j+\frac{1}{2}} \int_{t_j}^{t_{j+1}} e^{-\frac{(t_{j+1}-t)}{\lambda_1}} \cos\left(\frac{t}{\lambda_2}\right) dt \qquad (2.9a)$$

$$I_s^{j+1} = E\dot{\varepsilon}^{j+\frac{1}{2}} \int_{t_j}^{t_{j+1}} e^{-\frac{(t_{j+1}-t)}{\lambda_1}} \sin\left(\frac{t}{\lambda_2}\right) dt \qquad (2.9b)$$

The variables I_c and I_s in eqs. (2.9) can be explicitly integrated. The stress at time t_{n+1}, $\sigma(t_{n+1})$ then becomes a matter of summing the hereditary integrals over the previous time steps. This is much more computationally efficient than the numerical integration of the differential equation (2.5).

A great many WONDY computer runs simulating the plexiglass flyer and graphite/peek plate impact experiments in [6] were performed. Equations (2.5), (2.7) - (2.9) were used to model the dispersion effects in the graphite/peek plates. Several of the experiments were modeled in an attempt to determine the empircal constants λ_1, λ_2, γ_1 and γ_2 to sufficient accuracy for graphite/peek material. An important criteria was the matching as close as possible to the experiments of the plate backface particle velocity. Curve fitting to separate experiments produced too much scatter in the empircal constants. This indicated that the original dispersion assumption in the form of eq. (2.5) was not fully satisfactory.

In an attempt to improve the material model, the following viscoelastic type of constitutive law was postulated to account for dispersion:

$$\sigma(t) = H(t) \int_0^t \overline{G}(t-t')\,\dot{\varepsilon}(t)\,dt \qquad (2.10)$$

where

$$\overline{G}(t) = \gamma C_{11} + (1-\gamma) C_{11} e^{-0.05\left(\frac{t}{\tau}\right)} \cos\left(\frac{t}{\tau}\right) \qquad (2.11)$$

This constiutive model yielded slightly better results than the previous one - eqs. (2.5) and (2.7) - (2.9). In Table 2.1 the modeling of impact experiment no. 204 [6], which consisted of a plexiglass flyer and a graphite/peek plate, with WONDY is described. See Figure 3.4 for a description of the impact experiments. Figure 2.1 indicates the results. The predicted and experimental backface

particle velocity of the plate is shown in Figure 2.1a. In general, the agreement is very good, with some deterioration later in the simulation as might be expected. Figure 2.1b describes the predicted V_1 (thru thickness) damage in the plate. A value of 1 indicates total delamination.

Overall, the viscoelastic/dispersion constitutive law represented by eqs. (2.10) and (2.11) offered some improvement over the original dispersion model expressed by eq. (2.5). Curve fitting to separate experiments produced less scatter, but in general the results were not fully satisfactory - the constitutive model was just not robust enough.

In reference [4], the authors programmed the viscoelastic constiutive law discussed in [15] into WONDY, and modeled some of the impact experiments in [6] which consisted of plexiglass flyers and graphite/peek plates. Their results appear to be very good with less scatter among the numerical results for different flyer/plate thicknesses, initial velocities, etc. than was obtained in this report. This approach [4] will probably be incorporated in future 2D and 3D continuum damage work.

- 3.45 mm PMMA flyer at 93 m/s onto 25.83 mm Gr/PEEK target (both flyer and target 102 mm diameter).
- Mesh Size--215 zones in flyer and 1500 zones in target.
- Geometric dispersion-dissipation constitutive law
  $\sigma = H(t)\int_0^t G(t-t')\dot{\varepsilon}(x,t')\,dt$ with $G(t) = \gamma C_{11} + (1-\gamma)C_{11}e^{-0.5(t'/\tau)}\cos(t/\tau)$.
- Coupling between dispersion and compressive nonlinearity
  $\gamma = (\gamma_0 + \delta E)/(1+\delta E)$ where $\delta E = A \times (E_{Hugoniot} - E_{Linear})/E_{Linear}$.
- Dispersion properties τ=0.01 μsec, γ=0.7
- Coupling constant A=150.0
- Damage properties η_1=2.5 μsec, n_1=2, σ_{G0}=70 MPa where
  $\sigma_G = \sigma_{G0}(1 - V_1^2)$.

Table 2.1 Modeling of impact experiment no. 204 [6], plexiglass flyer and graphite/peek plate.

FIGURE 2.1

SPECIMEN NO. 204--PREDICTIONS AND COMPARISON WITH EXPERIMENT (PMMA AT 93 M/S ONTO GRAPHITE/PEEK)

a. Backface Particle Velocity--Prediction Compared with Experimental Data

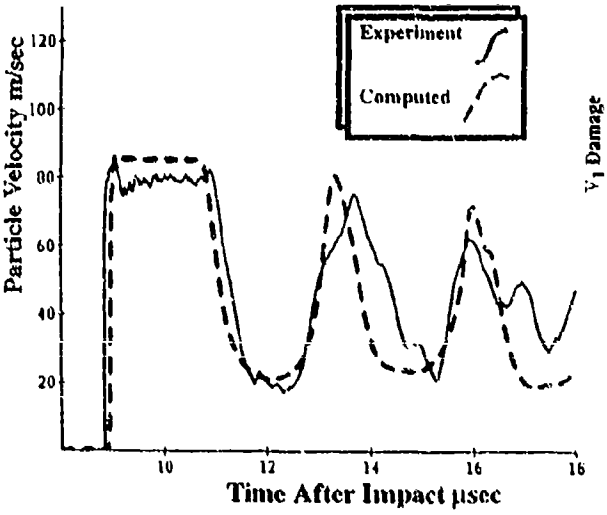

b. Predicted V_1 Damage

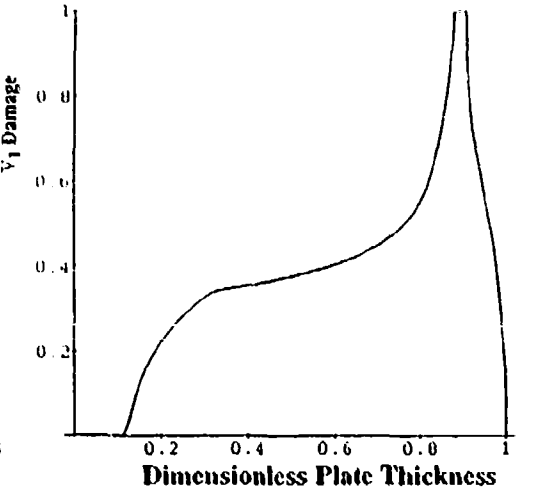

2.3 Predictions for composite plates subjected to underwater shock

In this section, the WONDY program is employed to predict the response of composite graphite/peek plates from 2 to 8 inches which are subjected to simulated near-field underwater explosions. Dispersion and damage are included in the material models used in the WONDY computer runs. The intent of these analyses is to assess the extent of spallation damage for various charge weights and ranges, and to determine the approximate boundaries of incipient and complete spallation. The history of a TNT explosive impulse passing through a fixed spatial point can be expressed as [21]:

$$p = p_0 e^{-\frac{t}{\theta}} \tag{2.10}$$

where p_0 is the pressure and θ the exponential decay constant. According to Aaron's law p_0 and θ can be determined using:

$$p_0 = 0.519 \left(\frac{W^{1/3}}{R}\right)^{1.13} \tag{2.11}$$

$$\theta = 0.925 \times 10^{-4} W^{1/3} \left(\frac{W^{1/3}}{R}\right)^{-0.22}$$

where p_0 is given in kilobars, θ is in seconds, R is the range in meters (m), and W is the charge mass in kilograms (kg). The values of W in eq. (2.11) will range from 5 kg to 30 kg, R will vary from .5 to 1.5 m (very close in), and the plates as previously stated will vary from 2 to 8 inches or .0508 to .1016 meters.

For seawater, the following material properties (SI units)are employed in the modeling:

$$\rho = 1000 \frac{kg}{m^3}$$
$$c_w = 1500 \frac{m}{s} \tag{2.12}$$
$$s_w = 1.75$$

where ρ is the density and c_0 is the bulk sound speed. The variable s comes from a linear shock velocity U_s to particle velocity U_p relationship of the form [7,8]:

$$U_s = c_w + s_w U_p \tag{2.13}$$

The material constants used for composite plates, which are assumed to be composed of graphite fibers and a peek matrix (see [6] and Appendix A) are as follows:

bulk properties

$$\rho = 1579 \frac{kg}{m^3} \tag{2.14a}$$

$$c_0 = 3000 \frac{m}{s}$$

$$E_{11} = 69.0 \times 10^9 Pa \text{ (thru thickness)}$$

$$E_{22} = 13.45 \times 10^9 Pa$$

$$\nu_{12} = 0.04, \ \nu_{13} = 0.3$$

damage parameters (see [1-3])

$$\eta_i = 1.0 \times 10^{-6}, \ N_1 = 1.0, \ \sigma_{G0} = 70 \times 10^6 Pa \tag{2.14b}$$

and the dispersion parameters (using the early dispersion model - see eq. (2.5))

$$\lambda_1 = - \ , \quad \lambda_2 = 5.0 \times 10^{-6}, \quad \gamma_1 = - \ , \text{and } \gamma_2 = 0.81 \tag{2.14c}$$

Figure 2.2 describes the WONDY model employed for the 2 inch thick plate and the fluid media. We note that the model for the fluid domain is only one half the thickness of the plate. In general it is desirable to include as little of the fluid as possible since the pressure wave, which is generated from a standoff position ranging from .5 to 1.5 meters in these analyses, must pass through the fluid on its way to the solid. The bulk sound speed of the fluid c_w is one half that of the composite c_0. Thus the time of flight ($=l/c$) is roughly the same for both the fluid and the composite media. In addition in these analyses, it was not necessary to employ silent boundary conditions [7,8] at point A of the fluid boundary. The analyses were terminated (the damage was done by the reflected tensile wave from the backface, point B, of the composite plate) before any spurious reflections from point A could reach the plate.

One other important point to be brought up with respect to Figure 2.2 concerns the number of finite difference zones used in the fluid and the composite plate. For the solid, 1000 zones were typically used to capture the damage and to accurately model the shock wave as it moved through the plate. This dicated the using of 500 zones in the fluid media. Employing zoning too coarse (with respect to the solid) in the fluid would result in the shock wave not being accurately propagated through the fluid. The selection of the time step δt is based upon the smallest l/c (l is the length of a zone) in the model, which for the model described in Figure 2.2 will be determined by the composite plate. Zoning too coarse in the fluid would not allow the shock wave to get across a zone in one time step and cause a diffusion of the wave.

In general, the use of 1500 zones in the finite difference meshes for this fluid-structure interaction problem would seem to be excessive. Based on the discussion in section 3.2 this may very well be the case. However, this point is not clear at this time and more modeling needs to be performed to determine minimum levels of discretization required to accurately model both the shock wave and the overall damage profile.

Finally in Figure 2.3, the results are shown for 2, 4 and 8 inch thich graphite/peek plates subjected to underwater explosions. Based on these predictions, it appears that spallation is not a real threat except for very close in explosions.

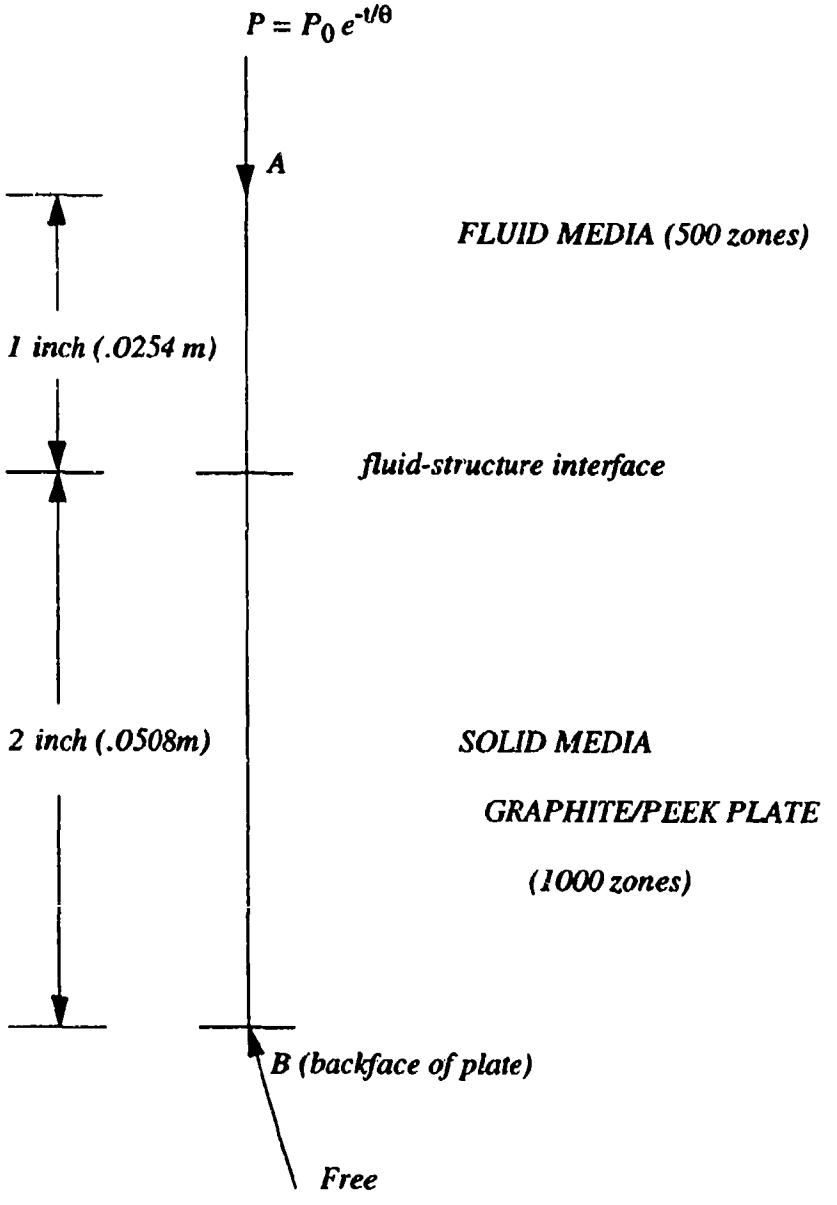

FIGURE 2.2 WONDY model for composite plate subjected to underwater shock.

FIGURE 2.3

EXPLOSION-INDUCED SPALLATION DAMAGE CALCULATIONS IN A CHARGE WEIGHT VS CHARGE RANGE SPACE FOR TNT IN WATER OVER GRAPHITE/PEEK

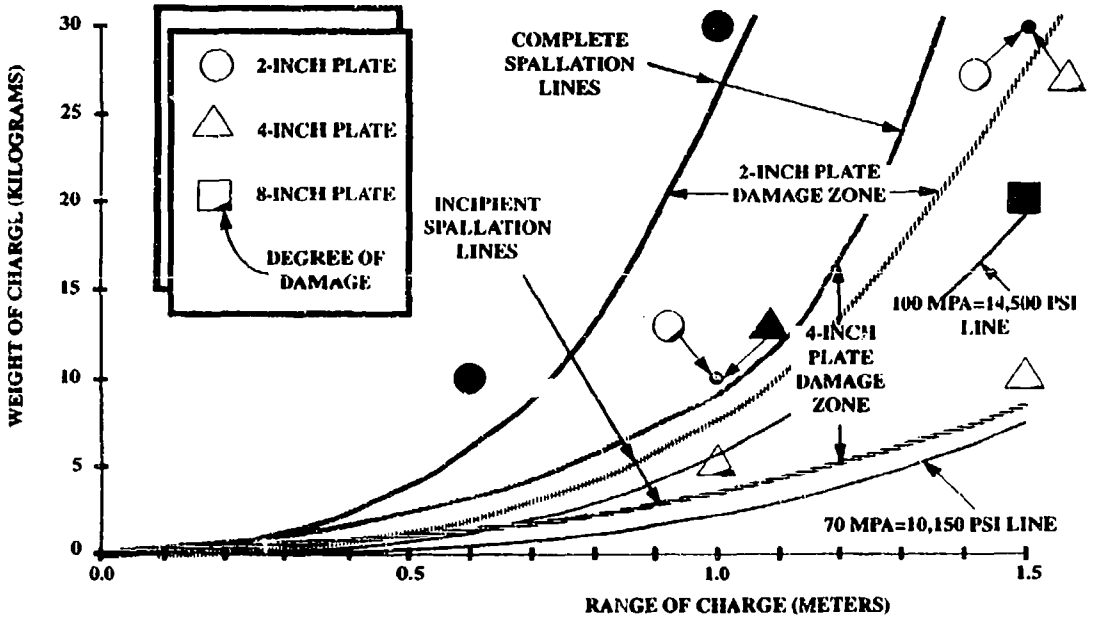

3. FURTHER APPLICATIONS OF THE 2D TRANSVERSELY ISOTROPIC CONTINUUM DAMAGE MODEL

3.1 Background

Details of the 2D transversely isotropic continuum damage model developed at NRL are contained in references [1-3]. Also, section 4.1 of this report briefly discusses some of the salient features of the 2D theory in developing a viable 3D continuum damage approach.

Basically our efforts to run detailed 2D continuum damage models with PRONTO2D have been hindered recently. We have begun the transition of the 2D and future 3D damage work away from PRONTO to the program ABAQUS/EXPLICIT [9]. This latter explicit finite element program has been developed by the architects of PRONTO. ABAQUS/EXPLICIT thus represents second generation software that possesses good pre- and post-processing capabilities, and is well documented and supported.

Another event that has hindered recent efforts to run detailed 2D damage models has been the retirement of the NRL CRAY-XMP, which was a COS machine. PRONTO2D was run in the past on this COS machine for larger jobs. A CRAY-EL is now available at NRL with the UNICOS operating system, but our development version of PRONTO2D could not be converted due to the COS libraries which are linked to the source code. Rather than trying to update a new UNICOS version of PRONTO2D, a decision was made to go completely to ABAQUS/EXPLICIT since it would be employed to develop 3D continuum damage capabilities. Appendix B is a listing of a user written subroutine for the current 2D damage theory being implemented into ABAQUS/EXPLICIT.

In the remainder of this section, we discuss PRONTO2D analyses which were run on a MicroVax, and are therefore limited in the fineness of the meshes and the number of elements allowed.

3.2 PRONTO2D comparisons to experimental and WONDY results

The intent of this section is to apply the 2D continuum damage theory of [1-3], which has been programmed into PRONTO2D, to a one dimensional (1D) impact problem that has been studied experimentally in [6] and with WONDY - see Figure 2.1 for results. As discussed in section 2.1 and Appendix A, the WONDY program is applicable to one dimensional situations, and contains both a reduced 1D damage model and a capability to account for dispersion/viscoelastic effects.

We address two questions in this section. The first concerns the effects of dispersion/viscoelasticity in the analyses, which is not explicitly included in the PRONTO2D model but is programmed into WONDY. The second question relates to the number of finite elements neededwith PRONTO2D (or ABAQUS/EXPLICIT) in the thru thickness direction to accurately predict the damage profile and the shock wave. Previous WONDY finite differnce runs had seemed to indicate that hundreds of finite difference zones were necessary to accurately simulate the shock wave thru the thickness of the plate. For instance, the WONDY results of Figure 2.1 employed 1500 zones thru the composite plate. For 2D and especially 3D problems, this would tranlate to hundreds of finite elements thru the thickness, and is completely impractical. Due to aspect ratio considerations, tens of thousands of elements would be required to model just a 2D plate and flyer.

With this in mind, we therefore focus upon the PRONTO2D modeling of impact experiment no. 204 in reference [6]. Table 2.1 and Figure 2.1 describe the WONDY modeling and results along with the experimental results for this impact problem, which consists of a plexiglass(PMMA) flyer and a graphite/peek plate of the same diameter. Because both the flyer and the plate are the same diameter, the early time response of the center of the plate can be approximated using a one dimensional model. Once bending and tranverse shear waves reach the center portion of the plate, this assumption is of course no longer valid. Table 3.1 indicates the material constants for the PMMA flyer along with the material and damage variables employed for the graphite/peek plate. (See also Figure 3.5, which indicates the material constants used in a typical PRONTO2D run. For

a further explaination of the variables used in the 2D continuum damage model programmed into PRONTO2D, refer to [1-3,8]). Two analyses are performed. Model A employs 100 elements thru the plexiglass flyer and 400 elements thru the graphite/peek plate. Model B is coarser and uses a quarter the number of elements, or 25 thru the flyer and 100 thru the composite plate. Also note that model B represents a viable mesh spacing in the thickness direction that could be extended for a true 2D model of this problem, including bending and shear effects that would arise later in the analysis. (See section 3.3 for a coarse 2D simulation of this problem with PRONTO2D.)

The PRONTO2D damage predictions for models A and B are indicated in Figures 3.2.1 and 3.2.2, respectively. Delamination damage in the plate is indicated in both figures. Comparing Figure 2.1 to these results, we see that model B (coarse mesh) produced damage predictions reasonably close to the very refined WONDY model (1500 zones). Model A with 400 elements thru the thickness of the plate was more ragged in the description of the total damage (V_1=1) than model B.

In general, the delamination results of models A and B indicate that the coarser mesh B compared better to the very refined WONDY model. At this point, it is thought that the coarser finite element (model B) may have compensated somewhat for the dispersion/viscoelasticity effects which are not included in PRONTO2D. (See also the comments concerning Figures 3.3.2 and 3.3.3). This is only speculation using at this point in time the WONDY results as the standard. In the future, comparison will be made to the data from ultrasound tests [6], and the forthcoming dissection of the plates.

In Figure 3.3.1, the predicted backface velocity of the plate from the coarse mesh, model B, is indicated. Comparing to the experimental results which are shown in Figure 2.1, one sees a good correlation. The peaks denoted by the points A, B, C, and D in Figure 3.3.1 match up very well with the experimental results. The width of the initial shock front, however, is narrower for the coarse PRONTO2D model and model B does not "shock up" as quickly as the experimental curve. Points E, F and G in Figure 3.3.1 also do not match up well with Figure 2.1. The predicted backface velocity is somewhat out of phase. Overall, however, the results of Figure 3.3.1 are very encouraging for our 2D (and 3D - section 4) continuum damage theories. The inclusion of viscoelas-

tic/dispersion capabilities should greatly assist in the closing of the gap between the experimental and predicted results, and offer a real hope in the modeling of 2D and 3D impact problems.

In Figure 3.3.2, the predicted backface velocity of the composite plate is shown for the fine mesh, model a (400 elements thru the thickness). Figure 3.3.3 displays the results from both model A and model B (coarse mesh). Comparing to the experimental results in Figure 2.1, we see that the fine mesh A "shocks up" quicker than mesh B. The initial shock front is also wider, and thus closer to the experimental results. However, past approximately 11 microseconds, the fine mesh predictions deteriorate and eventually around 18 microseconds severe oscillations are evident. (It is noted that with 400 elements thru the thickness of the plate, mesh A requires time steps approximately 1/4 those of mesh B to maintain stability based on the Courant criteria [8,9,23]. This can lead to accumulated error later in the time history, but should not cause such instability in general.)

Artificial viscosity [8] is contained in PRONTO2D to prevent high velocity gradients from collapsing an element before it can respond, and to help prevent oscillations or "ringing" such as seen in Figures 3.3.2 and 3.3.3. The following values for artiefical viscosity were used in obtaining the results shown in Figure 3.3.2:

$$b_1 = 0.1 \quad and \quad b_2 = 2.$$

where b_1 is the linear bulk viscosity coefficient and b_2 is the quadratic viscosity coefficient. As discussed in [8], b_1 helps to dissipate truncation frequency oscillations while b_2 is designed to smear a shock wave across several elements. In an attempt to decrease the oscillations, b_1 was next increased to .2, while b_2 was unchanged at 2. This choice of parameters produced even more severe oscillations in the predicted backface velocity of the plate. At this point, a final run was made using the PRONTO2D default values $b_1 = 0.06$ and $b_2 = 1.2$. Figure 3.3.4 describes the results for model A ($b_1 = 0.06$ and $b_2 = 1.2$) and model B which were obtained from Figure 3.3.1. The oscillations in the time history for the fine mesh , model A, have completely disappeared. It is evident that the later time results for the fine mesh, model A, are sensitive to the artificial viscosity parameters b_1 and b_2. Reference [23] contains a more thorough discussion of artificial viscosity. However at this time, we do not fully understand why the numerical oscillations

occurred for higher values of artificial viscosity.

The future inclusion of viscoelasticity/dispersion (see (2) in section 6, Future Directions) in the 2D and 3D continuum damage theories will provide additional damping that should help prevent such oscillations as in Figures 3.3.2 and 3.3.3. We note that the WONDY results, with up to 1500 zones in the composite plate, included dispersion in the formulation and this along with artificial viscosity helped to prevent the oscillations seen in some of the PRONTO2D models.

Overall, we conclude in this section that viscoelasticity/dispersion may have an important influence upon both the final damage profile, and in the capturing of the shock wave as it propagates thru the thickness of the composite plates. The approach discussed in [4] will be extended to 2D and 3D situations. With regards to the number of elements thru the thickness, it appears that a minimum of 100 may be required, but hundreds of elements are probably not necessary to achieve sufficient accuracy. Certainly more analyses still need to be performed before more definitive conclusions can be made. However, the results in this section are none the less quite encouraging.

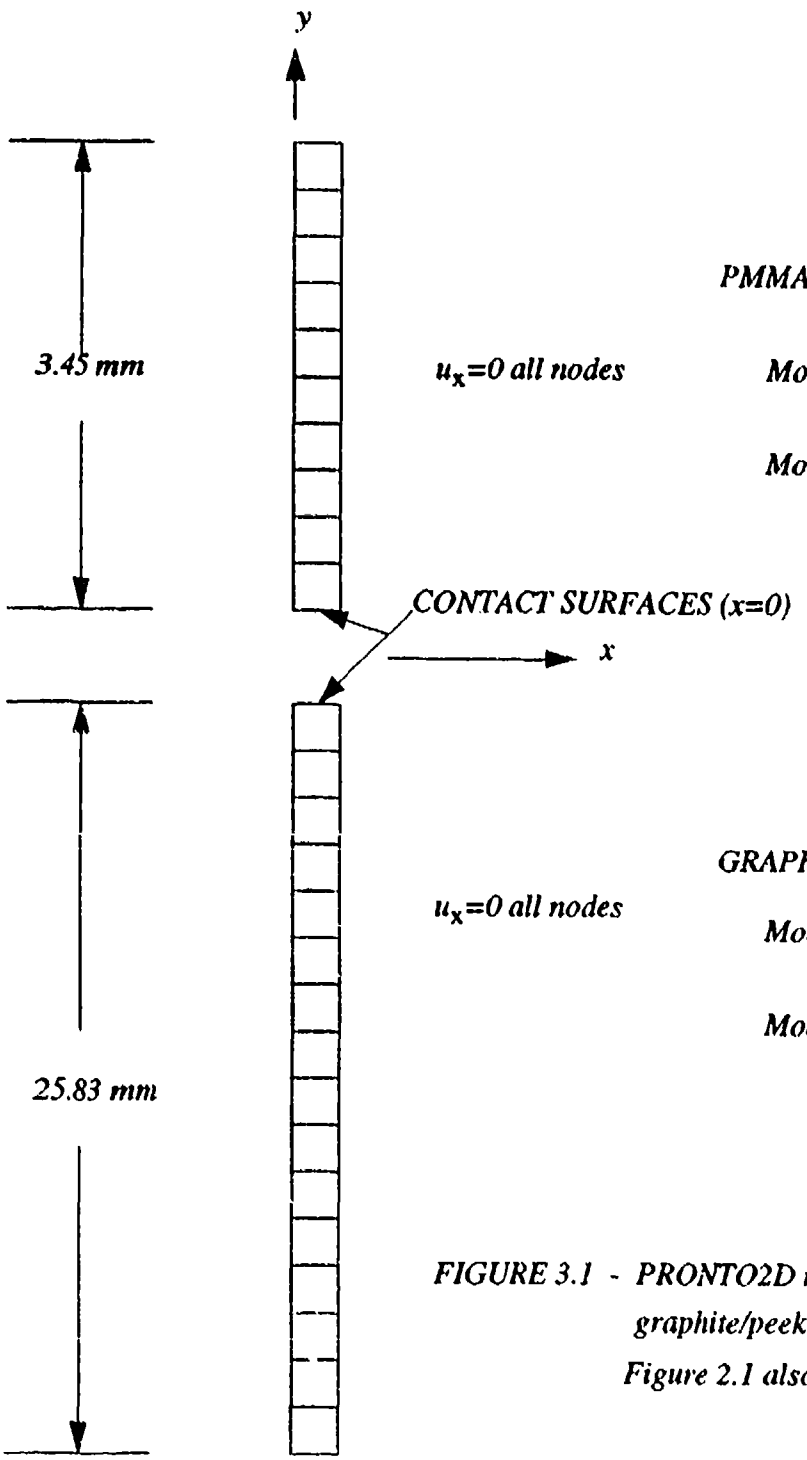

FIGURE 3.1 - PRONTO2D model of 1D impact of PMMA flyer and graphite/peek plate (specimen no. 204 in [6], see Figure 2.1 also).

TABLE 3.1 - Material and damage variables used for the PMMA flyer and the graphite/peek plate, in the PRONTO analyses - SI units.

PMMA (Plexiglass) Flyer

E (modulus) $= 9.595 \times 10^9$ Pa

ν (Poisson's ratio) $= .396$

ρ (density) $= 1185$ kg/m^3

Equation of State - Linear U_s- U_p Hugoniot form [8]

$U_s = C_0 + s\,U_p$

U_s= shock wave velocity, U_p = particle velocity

$C_0 = 2590.$ $s = 1.52$ Γ (Gruneisen ratio) = .97

GRAPHITE/PEEK PLATE

Material Properties

ρ (density)	$= 1579$ kg/m^3
E^0_{22} (planar modulus)	$= 69. \times 10^9$ Pa
E^0_{11} (thru thickness modulus)	$= 13.45 \times 10^9$ Pa
G^0_{12} (transverse shear modulus)	$= 7. \times 10^9$ Pa
ν_{12} (transverse plane)	$= .04$
ν_{23} (inplane)	$= .30$

Damage Parameters

$\alpha_1 = \alpha_2 = \alpha_3 = 0.75,$ $\alpha_4 = 0.95$

$\eta_1 = 2. \times 10^{-6},$ $n_1 = 2$

$\eta_2 = \eta_s = 1.4 \times 10^{-3},$ $n_2 = n_s = 1$

$\sigma_{G10} = 70. \times 10^6\ Pa$ $\tau_{G10} = 70. \times 10^6 Pa$

$\varphi_{G10} = 0.5,$ $\varphi_{G11} = 0.5$

$\sigma_{Gs0} = 170. \times 10^6 Pa$ $\tau_{Gs0} = 340. \times 10^6 Pa$

$\varphi_{G\cdot 0} = 1.,$ $\varphi_{GS1} = 1.$

Ultimate strain allowed

$\varepsilon_{ULT} = 0.015$

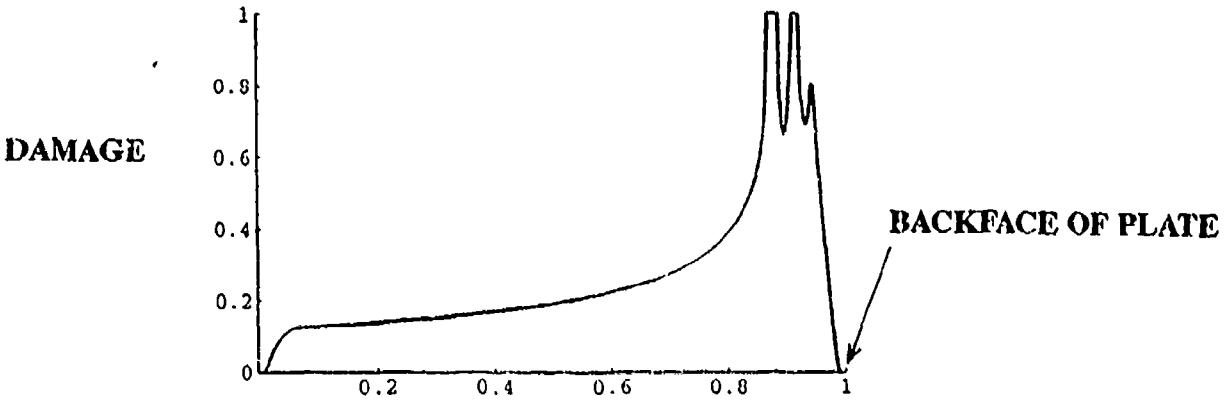

FIGURE 3.2.1 Model A, fine PRONTO2D mesh results.

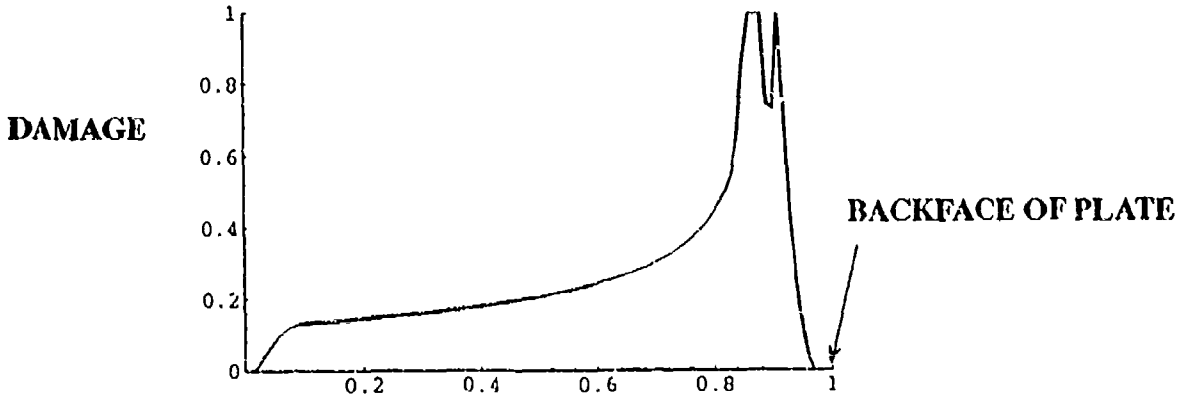

FIGURE 3.2.2 Model B, coarse PRONTO2D mesh results.

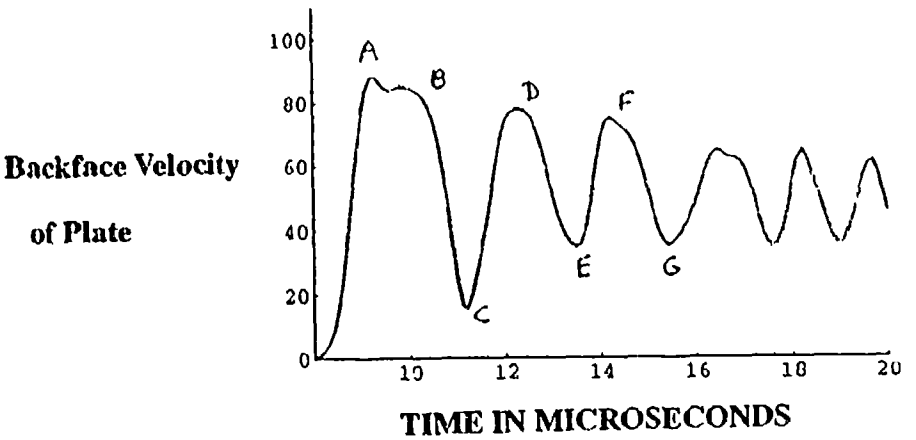

FIGURE 3.3.1 Predicted backface velocity of the plate for model B, coarse mesh

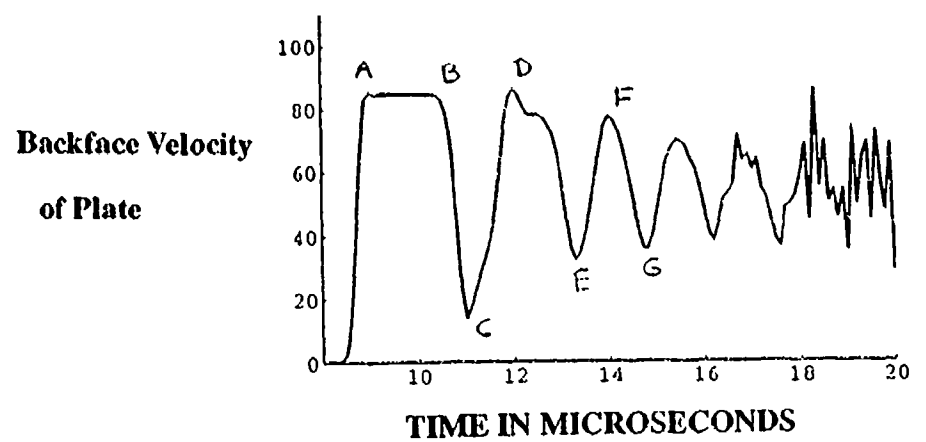

FIGURE 3.3.2 Predicted backface velocity of the plate for model A, fine mesh

—— Model A - 400 elements thru thickness, b_1=.1, b_2=2.

------ Model B - 100 elements thru thickness, b_1=.1, b_2=2.

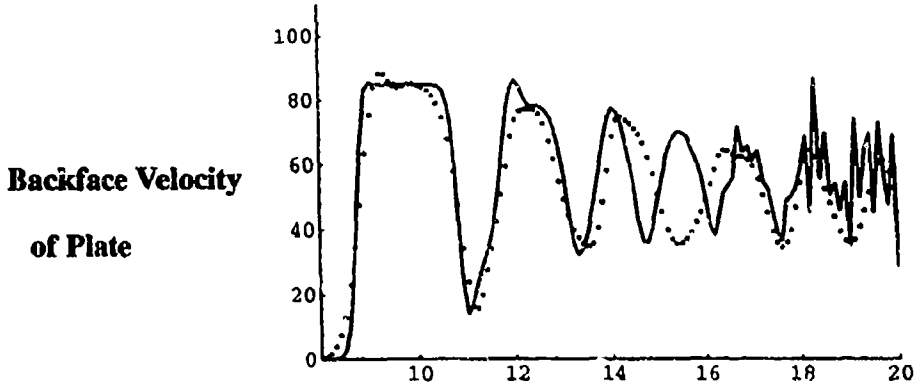

FIGURE 3.3.3 Predicted backface velocity of the plate for models A and B. Note oscillations in model A.

—— Model A - 400 elements thru thickness, b_1=.06, b_2=1.2

------ Model B - 100 elements thru thickness, b_1=.1, b_2=2.

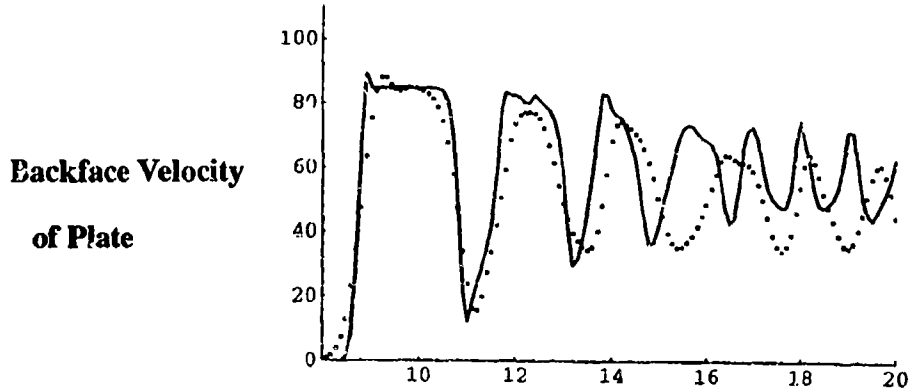

FIGURE 3.3.4 Predicted backface velocity of the plate for models A and B. No oscillations in model A.

3.3 Coarse model of 2D impact problem - circular PMMA flyer and graphite/ peek plate

Figure 3.4 describes the impact experiments that were conducted in [6], which consisted of axisymmetric PMMA (plexiglass) flyers impacting axisymmetric composite plates composed of either graphite/peek or graphite/epoxy. One dimensional models of experiment 204 are discussed in previous sections. See Table 2.1 and Figure 2.1 for WONDY model results, and Figures 3.3.1 and 3.3.4 for the PRONTO2D one dimensional simulation.

In this section, we will discuss the 2D modeling of the impact experiment using PRONTO2D and the 2D continuum damage model developed in [1-3]. In general, true 2D effects such as bending would become more prevailent at later time during the experiment and simulation. Early time predictions for the center of the plate would be dominated by one dimensional response - thus the use of one dimensional WONDY and PRONTO2D models in section 3.2. Figure 3.5 is a listing of the formatted PRONTO2D input. (Note nodal coordinates, element connectivity and boundary condition data are given in another input file and is unformatted for PRONTO2D). Material 1 in Figure 3.5 represents the graphite/peek plate, while material 2 is the PMMA flyer. The material and damage variables [1-3] for the graphite/peek plate are listed in Figure 3.5, and are the same as contained in Table 3.1. A very coarse PRONTO2D two dimensional model is indicated in Figure 3.6 in which 10 to 20 elements have been used thru the thickness of the flyer and composite plate. The PMMA flyer contains a total of 400 elements, while the graphite/peek composite plate is discretized with 800 elements.

In Figure 3.7, the predicted backface velocity of the centerline of the plate is plotted as a function of time. The experimentally measured plate backface velocity is given in Figure 2.1, along with WONDY predictions. In addition, PRONTO2D results for a 1D simulation using 100 and 400 elements thru the thickness of the plate are given in Figures 3.3.1 and 3.3.4. As one might expect with such a coarse 2D discretization, the PRONTO2D results of Figure 3.7 represent only a crude approximation. Figure 3.8 describes the PRONTO2D predicted thru thickness damage in the graphite/peek plate. Compare this result to Figure 2.1, which is from WONDY, and also to Figures

3.2.1 and 3.2.2 which represent PRONTO2D one dimensional models with 400 and 100 elements thru the thickness of the plate. In general, the damage results in Figure 3.8 are very approximate as expected.

Finally, it may perhaps appear odd to refer to Figure 3.6, in which 1200 elements (800 in the plate) have been employed, as a coarse mesh. However, one is trying to simulate impact experiments in very hetergeneous composite materials. Many degrees of freedom are required to accurately capture the shock wave as it progresses thru the media. Recall in section 3.2, model B (one dimensional simulation) with 100 PRONTO2D elements thru the thickness compared well to the early time experimental results for the backface velocity of the plate. More will be said in section 5, Summary and Future Directions, concerning discretization and also the inclusion of viscoelasticity/dispersion effects.

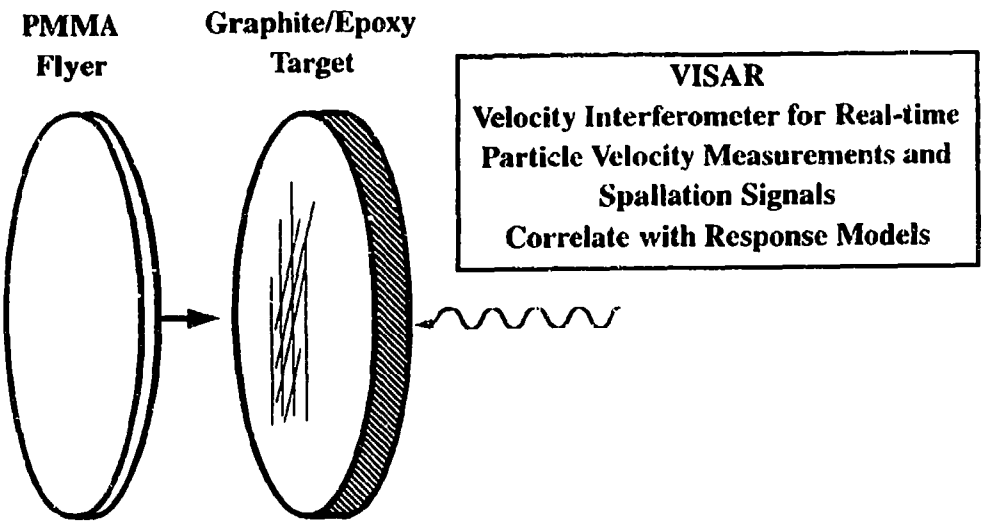

FIGURE 3.4 Impact tests conducted in [6].

```
TITLE
 LAST PROBLEM -PMMA FLYER,GR-PEEK PL.-SHOT 3357-1200EL.
PLANE STRAIN
BULK VISCOSITY=.1,2.
.ATERIAL,1,TRANS ISO W OAM,1579.
PLANAR MODULUS=69.E9
THRU MODULUS=13.45E9
NUTRANSPL=.04
NUINPLANE=.3
SHEARTRANS=7.0E9
A1=.75
A2=.75
A3=.75
A4=.95
ET1=2.E-06
N1=2.
ET2=1.4E-07
N2=1
V1SIGG0=70.E6
V1TAUG0=70.E6
V1PHIG0=.5
VLPHIG=.5
V2SIGG0=170.E6
V2TAUG0=340.E6
V2PHIG0=1.
VEPHIG=1.
EULT=.015
END
MATERIAL,2,EP HYDRODYNAMIC,1185.
YOUNGS MODULUS=9.595E9
POISONS RATIO=.396
YIELD STRESS=10.E10
HARDENING MODULUS=9.595E8
BETA=1.
PRESSURE CUTOFF=-1.E8
END
EQUATION OF STATE 2 = MG US-UP
C0=2590.,S=1.52,GAMMA=.97
END
NO DISPLACEMENT,X,1
INIT VEL MAT,2,0.,-93.
CONTACT SURFACE,100,200,.1,.5
TERMINATION TIME,25.E-6
OUTPUT TIME,1.E-7
PLOT TIME,1.E-7
PLOT NODAL=VELOCITY
PLOT ELEMENT,STRESS
PLOT STATE,V1,V2,DOUT
DEATH,1,DOUT,ABS,.99,.1
EXIT
(EOB)
```

FIGURE 3.5 PRONTO2D input for coarse model.

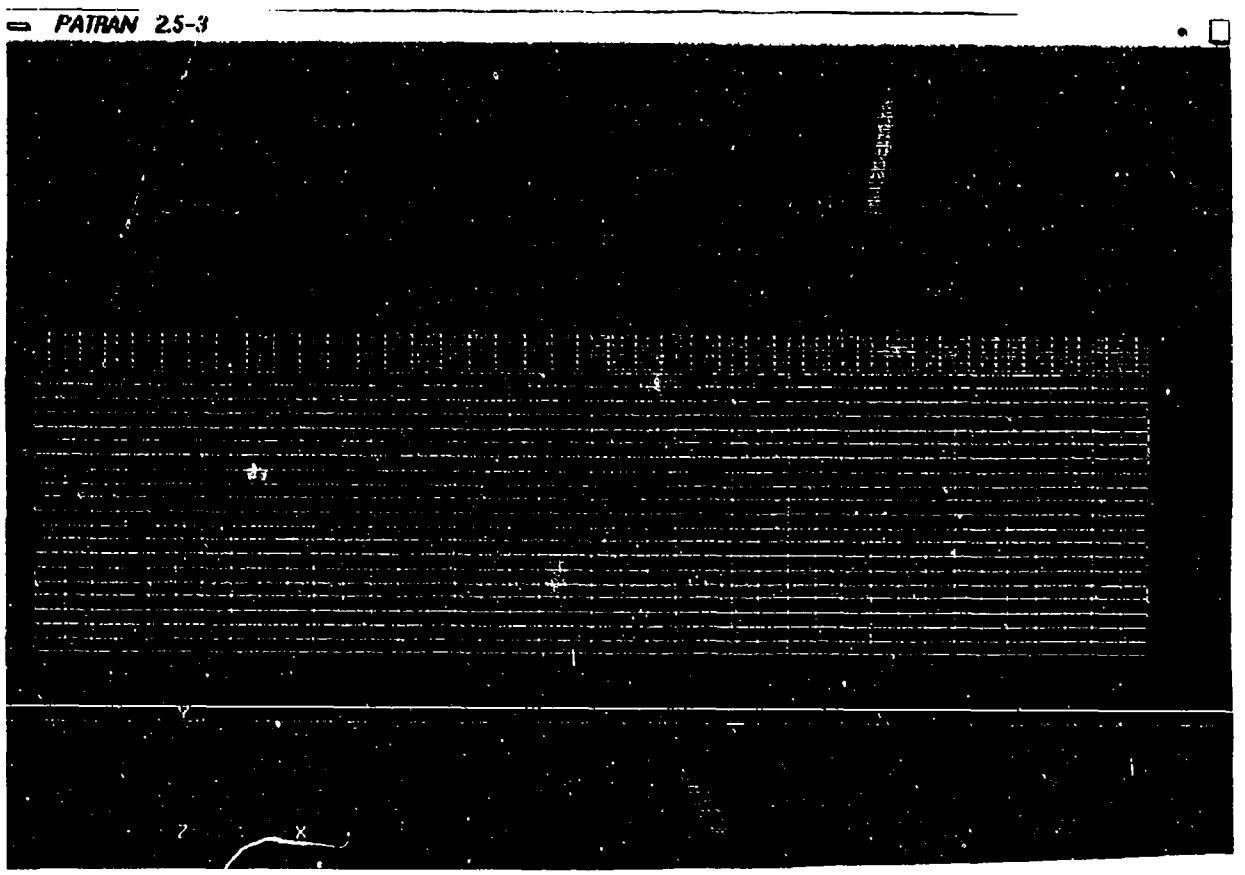

FLYER - .102 meters radius, .00345 meters thick, 10X40 elements

Plate - .102 meters radius, .02583 meters thick, 20X40 elements

FIGURE 3.6 Coarse PRONTO2D model of plexi-glass flyer and graphite/peek plate, impact vel. 93 m/s

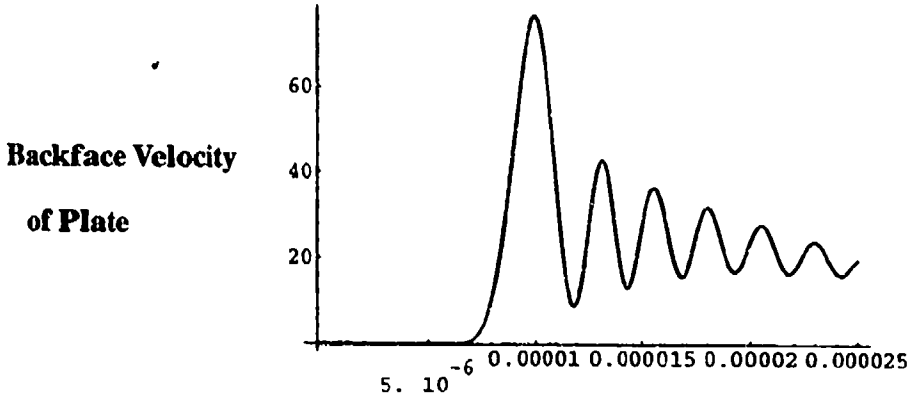

FIGURE 3.7 Centerline, backface particle velocity for the coarse PRONTO mesh in Fig. 3.6.

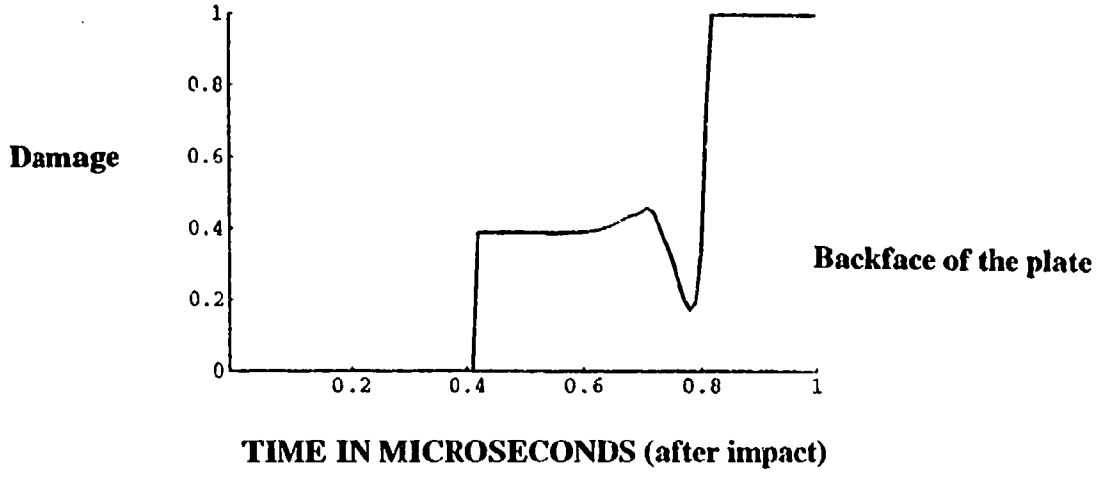

FIGURE 3.8 Thru thickness centerline damage prediction for the coarse PRONTO mesh in Fig. 3.6.

4. DEVELOPMENT OF A 3D CONTINUUM DAMAGE MODEL

4.1 General remarks

The development of a robust three dimensional (3D) continuum damage model for transient analysis of thick composites has proven to be a formidable task. A simple extension to the 2D theory, which is discussed in [1-3], is not viable. In what follows, a somewhat different approach for 3D continuum damage is developed.

Essentially, the 2D continuum damage model assumes transverse isotropy in the 1-2 plane as indicated in Figure 4.1. Delamination damage, representing a network of matrix cracking aligned in the 1-2 plane with normals in the 3 direction, is denoted by V_3 (V_1 in [1-3]) and depicted in Figure 4.2. Inplane matrix cracks, which may traverse or lie between reinforcing fibers but not break fibers, are indicated in Figure 4.3 and referred to as V_s damage in [1-3]. In this approach, damage effects were tracked and applied to the engineering moduli, shear moduli, and Poisson's ratios. Specifically for the coordinate system indicated in Figure 4.1, the following damage dependencies were assumed:

$$
\begin{aligned}
E_{33} &= (1 - V_3^2)\, E_{33}^0 \\
E_{11} &= E_{22} = (1 - \alpha_1 V_s^2)\, E_{11} \\
G_{31} &= (1 - V_3^2)\,(1 - \alpha_2 V_s^2)\, G_{31}^0 \\
\upsilon_{31} &= (1 - V_3^2)\,(1 - \alpha_3 V_s^2)\, \upsilon_{31}^0 \\
\upsilon_{12} &= (1 - \alpha_4 V_s^2)\, \upsilon_{12}^0
\end{aligned}
\qquad (4.1)
$$

where the superscript "0" denotes undamaged properties and the fractions $0 < \alpha_i < 1$, i =1, 4 are included to prevent a complete loss of material integrity as the saturation state $V \rightarrow 1$ is reached.

The assumption of transverse isotropy in the 2D formulation represents a reasonable approximation that allows the thru thickness direction to be more easily discretized. This approximation eliminates the requirement of tracking each individual ply and the various compliances associated

with them. It represents essentially a homogenization of the laminate. Note, however, a large number of elements are still required in the the 3 direction to accurately model transient thru thickness effects - see section 3.2.

In a 3D model of a laminated composite, the transverse isotropy assumption is no longer valid. Total damage, which will be represented by the vector $\underline{D}$, can be expressed by:

$$\underline{D} = D_1\underline{e}_1 + D_2\underline{e}_2 + D_3\underline{e}_3 \tag{4.2}$$

where $\underline{e}_i$ are unit base vectors and D_i are individual components of damage with normals aligned in the $\underline{e}_i$ direction.

A direct extension of the 2D damage model to 3D seems quite logical at first glance. However, this approach is very inefficient because it would necessitate the tracking of each individual ply and its compliances.

An alternate approach to the modeling of 3D damage is to track the damage and apply it to the stresses [10-12] as opposed to the compliances, as is done in the 2D model. In a one dimensional case, the effective stress $\bar{\sigma}$ with damage present can be related to the stress of the undamaged material by:

$$\bar{\sigma} = \sigma \times A/\bar{A} = \sigma/(1-D) \tag{4.3}$$

where

$$D = \frac{A-\bar{A}}{A} \tag{4.4}$$

is the scalar damage, and A is the original area, and $\bar{A}$ is the effective area due to material damage. From eq. (4.4), D is interpreted as the relative reduction in area caused by damage due to microcracking. For general anisotropic damage in three dimensions, the effective stress $\bar{\sigma}$ can be expressed in a tensorial form as:

$$\bar{\underline{\sigma}} = \underline{M}(\underline{D})\,\underline{\sigma} \tag{4.5}$$

where $\underline{M}$ is the second order material damage tensor and $\underline{D}$ is the damage vector defined by eq. (4.2). In references [10-12], the following form of $\underline{M}$ is proposed to account for anisotropic material damage in the principal coordinate system:

$$M = \begin{bmatrix} (1/(1-\alpha_1 D_1)) & 0 & 0 & 0 & 0 & 0 \\ 0 & (1/(1-\alpha_2 D_2)) & 0 & 0 & 0 & 0 \\ 0 & 0 & (1/(1-\alpha_3 D_3)) & 0 & 0 & 0 \\ 0 & 0 & 0 & \dfrac{1}{\sqrt{(1-\alpha_1 D_1)(1-\alpha_2 D_2)}} & 0 & 0 \\ 0 & 0 & 0 & 0 & \dfrac{1}{\sqrt{(1-\alpha_1 D_1)(1-\alpha_3 D_3)}} & 0 \\ 0 & 0 & 0 & 0 & 0 & \dfrac{1}{\sqrt{(1-\alpha_2 D_2)(1-\alpha_3 D_3)}} \end{bmatrix} \tag{4.6}$$

where, as in the 2D damage theory, the fractions $0 < \alpha_i < 1$, i -1,2,3 have been added to prevent a complete loss of material integrity as the individual components of damage D_i go to 1.

For individual plies, eqs. (4.5) and (4.6) can be easily applied, since the principal directions are in the 1-2 plane (see Figure 4.1) and are parallel and perpendicular to it. Then the stress tensor $\underline{\sigma}$ can be transformed to the global 1-2 axes. In this work, we will apply eqs. (4.5) and (4.6) to groups of plies, and assume the additional approximation that the global 1-2 axes represent the principal axes (see comments at the end of this section).

For linear elasticity, the relationship between the stress and the strain tensors can be written as:

$$\underline{\sigma} = \underline{C}\underline{\varepsilon} \tag{4.7}$$

where $\underline{C}$ is the constitutive tensor and $\underline{\varepsilon}$ is the strain. In the case of an orthotropic lamina in which there is no interaction between the shear stress, eq. (4.7) is of the form [22]:

$$\begin{bmatrix} \sigma_{11} \\ \sigma_{22} \\ \sigma_{33} \\ \sigma_{12} \\ \sigma_{13} \\ \sigma_{23} \end{bmatrix} = \begin{bmatrix} C_{11} & C_{12} & C_{13} & 0 & 0 & 0 \\ C_{21} & C_{22} & C_{23} & 0 & 0 & 0 \\ C_{31} & C_{32} & C_{33} & 0 & 0 & 0 \\ 0 & 0 & 0 & C_{44} & 0 & 0 \\ 0 & 0 & 0 & 0 & C_{55} & 0 \\ 0 & 0 & 0 & 0 & 0 & C_{23} \end{bmatrix} \begin{bmatrix} \varepsilon_{11} \\ \varepsilon_{22} \\ \varepsilon_{33} \\ \varepsilon_{33} \\ \varepsilon_{13} \\ \varepsilon_{23} \end{bmatrix} \tag{4.8}$$

where 1,2, and 3 are the principal axes. In terms of the engineering constants, the components of the constitutive tensor $\underline{C}$ are:

$$\begin{aligned} C_{11} &= (1-\nu_{23}\nu_{23})/(E_2E_3\beta) \\ C_{12} &= (\nu_{12}+\nu_{32}\nu_{13})/(E_1E_3\beta) = C_{21} \\ C_{13} &= (\nu_{13}+\nu_{12}\nu_{23})/(E_1E_2\beta) = C_{31} \\ C_{22} &= (1-\nu_{13}\nu_{31})/(E_1E_3\beta) \\ C_{23} &= (\nu_{23}+\nu_{21}\nu_{13})/(E_1E_2\beta) = C_{32} \\ C_{33} &= (1-\nu_{12}\nu_{21})/(E_1E_2\beta) \\ C_{44} &= G_{12}, \qquad C_{55} = G_{13}, \qquad C_{66} = G_{23} \end{aligned} \tag{4.9}$$

and

$$\beta = (1-\nu_{12}\nu_{21}-\nu_{23}\nu_{32}-\nu_{31}\nu_{13}-2\nu_{21}\nu_{32}\nu_{13})/(E_1E_2E_3)$$

where ν_{ij}, E_i and G_i represent the various Poisson ratios, the engineering and shear moduli. In addition, there is also the following relationship:

$$\nu_{ij}/E_i = \nu_{ji}/E_j \tag{4.10}$$

where the summation convention is suspended.

Equations (4.8) and (4.9) can be constructed for each individual ply. However as discussed previously, it is not our intent to track the damage in each ply but rather in groups of plies. This latter approach allows more flexibility in the discretization of the thru thickness direction (3 axis). For 3D and 2D solid finite element, explicit transient analysis, such as the programs PRONTO2D [8] and ABAQUS/EXPLICIT [9], employ linear solid elements with reduced or one point integration. With this in mind, equations (4.7) - (4.10) can be applied to groups of plies and their effect incorporated into a single element. Within a linear element due to one point integration, the stress and strain do not vary in the thru thickness direction (or in the other two directions). Thus, eq. (4.7) for a group of N plies can be written as:

$$\underline{\sigma} = \sum_{i=1}^{N} \underline{C}_i \underline{\varepsilon} \tag{4.11}$$

In lumping together groups of plies with orientations a,b,c,d for instance, we appear to be restricting the number of element allowed in the 3 direction. As discussed in sections 2 of this report, in many instances over 100 elements thru the thickness may be required to track the wave nature of the response. If there are only 10 groups of plies with orientations of a,b,c,d, with this approach only 40 elements in the 3 direction could be allowed before individual plies would have to be modeled with more than one element. This approach would be very difficult particularly with respect to pre-processing. To overcome thus defficiency, an additional approximattion is introduced, which assumes each group of plies can be broken down into subgroups with exactly the same group of plies as the original group a,b,c,d, but with scaled thicknesses. Thus, if as in this case, there are 10 groups of plies with orientations of a,b,c,d and 100 elements thru the thickness are required, it is assumed that there are 100 groups of plies (a,b,c,d) with thickness 1/10 of the original layup. This latter homogenization approximation appears to be a reasonable compromise to the modeling of each individual ply, or the possibility of requiring more than one element per ply should additional elements be necessary in the 3 direction.

We return now to equations (4.5) and (4.6). The strain energy W of an undamaged material can be expressed as:

$$W = \frac{1}{2}\sigma^T\varepsilon \tag{4.12}$$

Using eq. (4.7), (4.12) becomes:

$$W = \frac{1}{2}\varepsilon^T C\varepsilon \tag{4.13a}$$

in terms of the strain tensor ε or

$$W = \frac{1}{2}\sigma^T C^{-1}\sigma \tag{4.13b}$$

with respect to the stress. The strain energy W_D for a damaged material is expressed as [10]:

$$W_D = \frac{1}{2}\bar{\sigma}^T C^{-1}\bar{\sigma} \tag{4.14}$$

Using eq. (4.5) produces:

$$W_D = \frac{1}{2}\sigma^T (M^T C^{-1} M)\,\sigma$$

or

$$W_D = \frac{1}{2}\sigma^T \bar{C}^{-1}\sigma$$

where

$$\bar{C}^{-1} = M^T C^{-1} M \tag{4.15}$$

Inverting eq. (4.15) produces the damaged constitutive tensor:

$$\bar{C} = M^{-1} C (M^T)^{-1} \tag{4.16}$$

Because of eq (4.6), M is assumed to be a diagonal matrix, and thus its inverse is easy to obtain.

Before closing this section, we return to eqs. (4.5) and (4.6). The M matrix is assumed to be diagonal, and also referenced to the principal coordinate system. In general for laminated composites, the 1 and 2 directions will not correspond to the principal directions This assumption, however, can be partially rectified by adjusting the thresholds (see section 4.2) for damage to more accurately reflect the grouping of the individual plies within a single finite element.

4.2 Details of the damage model

Having postulated an approach to model 3D continuum damage in a thick composite, we next describe the specific details of the damage model. The intended application is for composite materials which usually contain a great number of imperfection sites from which cracks can grow. Thus, the nucleation of new cracks is not addressed. Rather, the focus is on the growth and evolution of damage.

Recall from eq. (4.2) that the damage D is assumed to be a vector with components D_i in the 1, 2, and 3 directions. As in the 2D model [1-3], the evolution of the individual components of damage are assumed to be governed by a threshold in the form:

$$\begin{aligned} F_i(\sigma, f_i(D_j)) \quad &\leq 0 \qquad \textit{for no damage growth} \\ &> 0 \qquad \textit{for damage growth} \end{aligned} \tag{4.17}$$

where (i,j)=1,2,3 and there is no sum on i; F_i are scalar threshold functions; σ is the current stress tensor; and f_i is an array of current threshold parameters which are functions of D_j, the damage component. F_i is assumed, as in [1-3], to be of the Mohr-Coulomb type and to be dependent upon the stress measures σ_t and τ (tension and shear) as follows:

$$F_i(\sigma_t, \tau, f) = \left(1 + \left(\frac{\tau}{f_{3i}}\right)^2\right)^{1/2} - (f_{1i} - \sigma_t)/f_{2i} \tag{4.18}$$

In eq. (4.18) the parameters are related to specific growth threshold strengths σ_{Gi} and τ_{Gi}, and the Coulomb friction tangent ϕ_{Gi} as:

$$\begin{aligned} \sigma_{Gi} &= f_{1i} - f_{2i} \\ \tau_{Gi} &= f_{3i}\left((f_{1i}/f_{2i})^2 - 1\right)^{1/2} \\ \phi_{Gi} &= f_{3i}/f_{2i} \end{aligned} \tag{4.19}$$

The tension and shear growth thresholds as well as the Coulomb friction tangent in eqs. (4.19) are assumed to be functions of the damage D_i. The threshold surface ($F = 0$)defined by eq. (4.18) is

shown in Figure 4.4 along with the various parameters. Note that in this figure d is the shortest distance fron an external state (σ_t, τ) to the threshold surface.

Using eqs. (4.18) and (4.19), we further develop the details for the components of damage D_i and its evolution. For D_3 type of damage, which corresponds to delamination, the stress measures σ_{ti} and τ_i, are postulated to be of the form:

$$\begin{aligned} \sigma_{t3} &= \sigma_{33} \\ \tau_3 &= (\sigma_{31}^2 + \sigma_{32}^2)^{1/2} \end{aligned} \tag{4.20}$$

The growth threshold stresses and the Coulomb friction tangent in eqs. (4.19) are then taken to be:

$$\begin{aligned} \sigma_{G3} &= (1 - D_3^2)\,\sigma_{G30} \\ \tau_{G3} &= (1 - D_3^2)\,\tau_{G30} \\ \varphi_{G3} &= \varphi_{G30} + D_3^2\,(\varphi_{G31} - \phi_{G30}) \end{aligned} \tag{4.21}$$

where the "0" subscript denotes the initial undamaged properties. Note that for σ_{G3} and τ_{G3} all resistance to damage is lost as D_3 goes to 1; and the Coulomb friction tangent φ_{G1} can vary linearly with D_3^2 as the damage progresses.

From eqs. (4.18), (4.19), the variables f_{23}, f_{13} and f_{33} are:

$$\begin{aligned} f_{23} &= \frac{1}{2}\left(\frac{\tau_{G3}^2}{\phi_{G1}^2 \sigma_{G3}} - \sigma_{G3}\right) \\ f_{13} &= \sigma_{G3} + f_{23} \\ f_{33} &= f_2 \varphi_{G3} \end{aligned} \tag{4.22}$$

To complete the continuum damage formulation for D_3 damage, evolution equations are required. From [1-2], the following relationship is postulated for D_3 (delamination) damage:

$$\frac{dD_3}{dt} = \bar{F}_3(d_3, D_3) \tag{4.23}$$

where d_3 is the shortest distance in the σ_t, τ stress space (eq. (4.20)) - see Figure 4.4 for the threshold surface $F = 0$. For $d_3 = 0$, $F = 0$ and $\frac{dD_3}{dt} = 0$ for all stress points interior or on the thresh-

old surface ($F = 0$). The specific form of eq. (4.23) employed in [1-2] and which will be used here is expressed as:

$$\frac{dD_3}{dt} = (d_3/\sigma_{G30})^{n_3}/(\eta_3(1-D_3^2)) \tag{4.24}$$

where n_3 is a positive power exponent for d_3/σ_{G30} (a dimensionless stress distance), η_3 is a time constant governing the rate, and the term $1/(1-D_3^2)$ causes an acceleration of the damage to complete delamination as D_3 goes to 1.

Next we consider D_1 and D_2 type of damage, which relate to matrix cracking. The discussion will focus on D_1, but D_2 type of damage will be assumed to be of the same form. The substituion of 2 for the index 1 in the equations to follow will yield the D_2 formulation. For D_1 type of damage, the stress measures σ_{t1} and τ_1 required for eqs. (4.18) and (4.19) are postulated to be of the form:

$$\begin{aligned} \sigma_{t1} &= \sigma_{11} \\ \tau_1 &= (\sigma_{12}^2 + \sigma_{13}^2)^{1/2} \end{aligned} \tag{4.25}$$

Equations (4.25) are used in conjunction with eqs. (4.18) and (4.19). The form of the growth threshold stresses is not of the same form as D_3 damage, which is given by eq. (4.19). D_1 (and also D_2) damage consists of an ever denser network of cracks which tend to saturate. There is no acceleration to a catastrophic failure as in the case of D_3 damage which represents delamination. Saturation can be forced through the growth thresholds as done in [1-2]:

$$\begin{aligned} \sigma_{G1} &= \sigma_{G10}/(1-D_1^2) \\ \tau_{G1} &= \tau_{G10}/(1-D_1^2) \end{aligned} \tag{4.26}$$

while Coulomb friction tangent is taken to be

$$\varphi_{G1} = \varphi_{G10} + D_1^2(\varphi_{G11} - \varphi_{G10}) \tag{4.27}$$

In eq. (4.26) it is seen that as D_1 goes to 1 damage becomes more difficult since the growth thresholds σ_{G1} and τ_{G1} greatly increase. Reference [1] also offers another form for the threshold functions - see that discussion for further details.

For D_1 (and D_2) damage, the final ingredient required is the specific form of the rate evolution equation which is described by eq. (4.23). Since there is no acceleration to a catastropic failure, as in the case for D_3 damage, a viable form is taken to be:

$$\frac{dD_1}{dt} = (d_1/\sigma_{G10})^{n_1}/\eta_1 \qquad (4.28)$$

where as in eq. (4.24) η_1 is a time constant, d_1 is normalized with the virgin growth threshold stress σ_{G10}, and n_1 is a positive term for the dimensionless stress distance.

Another mode of continuum damage is the breakage of the reinforcing fibers. To account for this effect, a simple maximum strain criteria is used in the 3D model. The D_1, D_2 and D_3 forms of damage cause softening of the composite response and thus directly influence this maximum strain criteria.

In closing this section, it is noted that at the time this report is being written, the 3D continuum damage model is being programmed as a user written subroutine for ABAQUS/EXPLICIT.

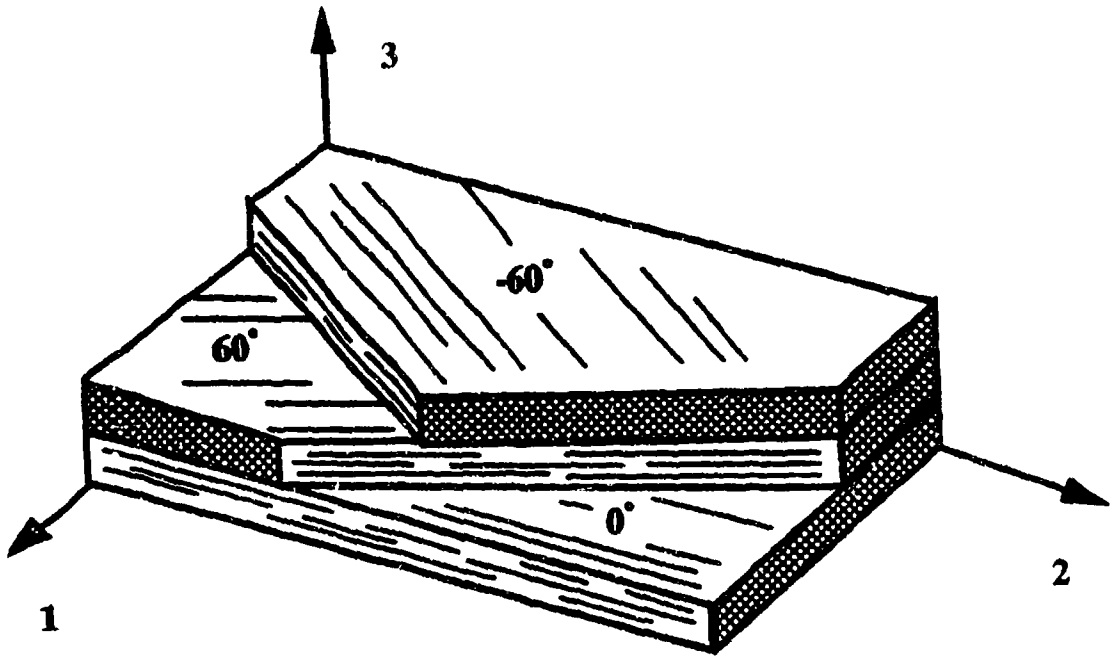

FIGURE 4.1. Portion of a 0 deg, + and - 60 deg ply layup.

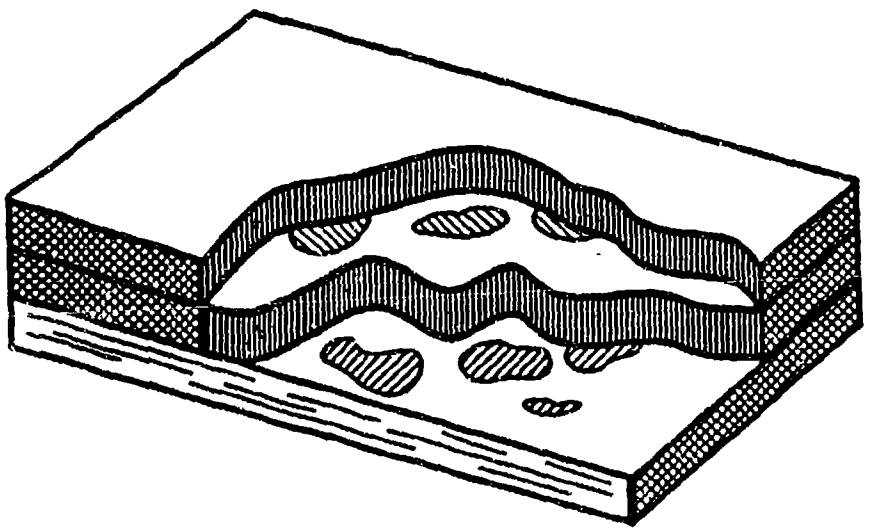

FIGURE 4.2 V_3 delamination damage.

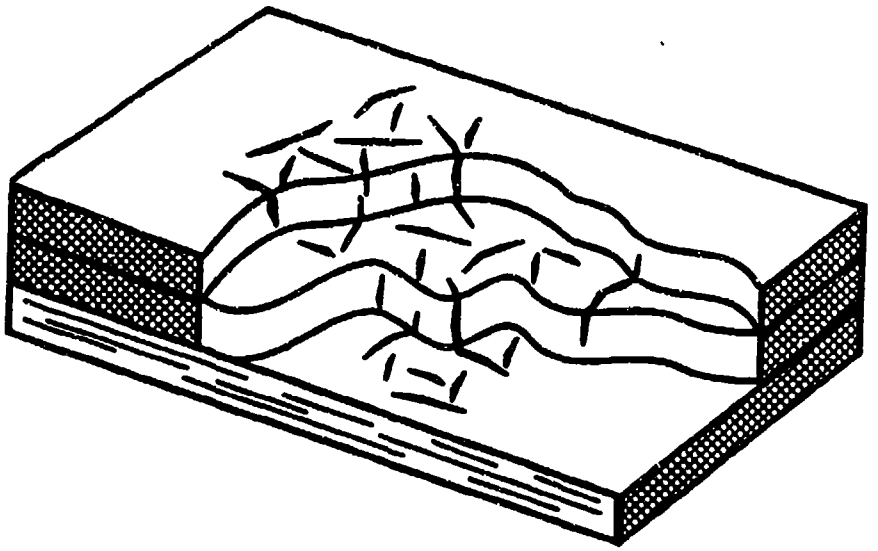

FIGURE 4.3 V_S inplane matrix damage.

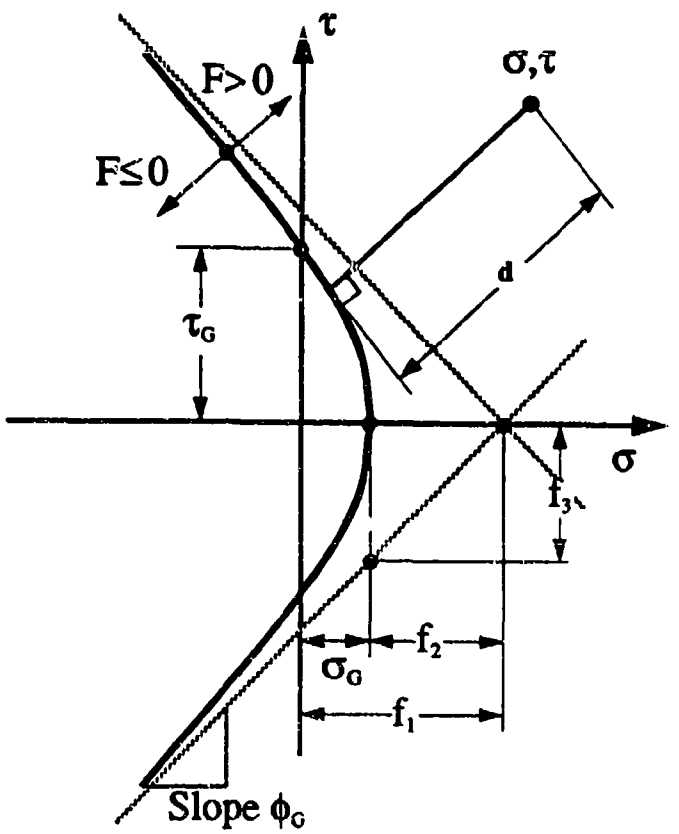

FIGURE 4.4 Threshold surface for the onset of damage.

5. SUMMARY AND CONCLUSIONS

The results of this report document progress made in predicting the early time response of thick composite plates subjected to multi-dimensional shock loading. In general, numerical predictions compare very well to available experimental data. Overall, the results of this report are very encouraging for the 1D, 2D and 3D continuum damage theories developed at NRL for the evolution of damage in thick composite shell structures.

Dispersion effects in a 1D damage model are discussed in section 2. An approach is developed that employs higher order derivatives in the constitutive relations. This is shown to be equivalent to a viscoelastic theory. This approach has been programmed into the one dimensional finite difference program WONDY. Comparisons to experimental results were good. However, this approach required too much curve fitting of data from individual experiments and was not robust enough. The use of a more straightforward viscoelasticty theory [15] in WONDY along with the 1D damage theory proved to be superior and is documented in [4].

In section 2.3, using the WONDY program with dispersion and damage included, 1D damage predictions are made for thick composite plates subjected to underwater shock. Based on these results, it appears that spallation is not a real threat except for very close in explosions.

In section 3, PRONTO2D finite element models containing the 2D transversely isotropic continuum damage theory are compared to experimental and WONDY results for the impact of plexiglass flyers onto graphite/peek plates. Plate backface velocity predictions from the 1D PRONTO2D models compared very well to experimental measurements [6] and very finely discretized WONDY models which also contained viscoelasticty/dispersion. One hundred 4 node solid elements appear to be sufficient to capture the magnitude and the general shape of the shock wave. The inclusion into the 2D continuum damage theory of viscoelasticty as used in [4] as well as nonlinear elasticity in the thru thickness direction, should improve these results further - see section 6 item (2) for additional comments.

A new 3D continuum damage theory is developed in section 4 for thick laminated composite

plates. The 3D theory represents, in part, an extension of the 2D transversely isotropic damage theory contained in [1-3]. However, three dimensional considerations as well as the inefficiencies of modeling individual plies in a thick composite required a slightly different approach. A 3D formulation is developed which applies the damage vector $\underline{D}$ directly to the stresses, rather than the compliances as in the 2D theory. In general, this new 3D damage theory appears to be quite promising, offering real potential for more efficient and accurate modeling of thick laminated composite plates subjected to very transient loadings, such as impact and underwater shock.

6. FUTURE DIRECTIONS

Based on the success of our efforts at NRL to date concerning the development of numerical capabilities for predicting the response of thick composite shells subjected to very transient loadings, we plan to pursue the following directions.

(1) The 2D transversely isotropic continuum damage theory [1-3] will be implemented into ABAQUS/EXPLICIT. This capability will be used to model several of the experimental impact problems discussed in [6] in which plexiglass flyers were fired at thick graphite/peek plates and graphite/epoxy plates. Up to 100 elements thru the thickness will be employed. True 2D problems in which the diameter of the flyer is smaller than the plate (edge effects) as well as bending and transverse shear effects (later time) will be investigated. Direct comparisons to the experimental data in [6] will be made, especially plate backface velocity histories. In addition, damage predictions will be compared to any available data such as contained in [5].

(2) Viscoelasticity is important in the response of composite plates to dynamic loading. Therefore, a viscoelastic formulation similar to [15,4] will be incorporated into the 2D continuum damage theory and implemented into ABAQUS/EXPLICIT. This formulation will of course also introduce dispersion into the composite. Also included will be nonlinear elasticity in the normal or thru thickness direction of the plate.

(3) The new 3D continuum damage theory, developed in section 4 of this report, will be fully implemented into ABAQUS/EXPLICIT. Viscoelasticity and nonlinear elasticity in the thru thickness direction of the plate will also be introduced.

(4) A new thick plate/shell continuum damage theory based upon the new 3D theory of section 4 will be developed.

(5) We will begin to investigate the introduction of the 2D and 3D continuum damage theories into an implicit FEM program such as ABAQUS/STANDARD. Implicit codes have

typically been much more useful than explicit programs for structural dynamics types of problems, such as underwater shock, in which one is not trying to track the actual wave propagation in the structure. Projectile impact types of problems, on the other hand, are an example best modeled usually with an explicit program. Implicit approaches require the formulation, computation and inverse of a global stiffness matrix, but can use much larger time steps and are usually unconditionally stable. The integration of the governing constitutive relations is also usually more involved in implicit formulations.

Acknowledgement

This work was supported by the DARPA Naval Technology Office, and that support is greatly appreciated.

7. REFERENCES

1) J. A. Nemes and P. W. Randles, Modelling the Response of Thick Composite Materials Due to Axisymmetric Shock Loading, NRL Memorandum Report 6856, August 5, 1991.

2) P. W. Randles and J. A. Nemes, A Continuum Damage Model for Thick Composite Materials Subjected to High-Rate Dynamic Loading, Mechanics of Materials, Volume 13, No. 1, 1992.

3) J. A. Nemes and P. W. Randles, A Constitutive Damage Model for Composite Materials Subjected to High-Rate Loading, in Constitutive Laws for Engineering Materials, edited by C. S. Desai, E. Kremple et al, ASME Press, Jan. 1991.

4) J. A. Nemes and P. W. Randles, in preparation.

5) K. Simmonds, P. W. Randles and T. Whitcombe, Assessment of Impact Damage in Thick Graphite/Epoxy and Graphite/Peek Composites, NRL Memorandum Report, in preparation.

6) E. A. Smith, Shock Response of Two Thick Composites GR-EP and GR-PEEK, Ktech Corporation, KTECH/TR-91/02, Albuquerque, NM, August 1991.

7) M. E. Kipp and R. J. Lawrence, WONDY 5 - A One Dimensional Finite Difference Wave Progation Code, SANDIA Report, SAND81-0930.UC-32, June 1982.

8) L. M. Taylor and D. P. Flanagan, PRONTO2D A Two Dimensional Transient Solid Dynamic Program, SANDIA Report SAND86-0594.UC-32, March 1987.

9) ABAQUS/EXPLICIT, (1) User's Manual and (2) Examples Manual, versions 5.1, Hibbittt, Karlsson and Sorensen, Inc., Pawtucket, R. I., 1992.

10) C. L. Chow and J. Wang, An Anisotropic Theory of Continuum Damage Mechanics for Ductile Fracture, Engineering Fracture Mechanics, Vol. 27, No. 5, pp. 547-558, 1987.

11) C. L. Chow and J. Wang, An Anisotropic Theory of Elasticity for Continuum Damage Mechanics, International Journal of Fracture 33, pp. 3-16, 1987.

12) J. Wang and C. L. Chow, A Non-proportional Loading Finite Element Analysis of Continuum Damage Mechanics for Ductile Fracture, Intern. Jour. Num. Meth. Engin., Vol. 29, pp. 197-209, 1990.

13) R. M. Christensen, Mechanics of Composite Materials, Chapter 7:, Wave Propagation, Wiley, 1979.

14) H. L. Schreyer, Chapter 6: Dispersion of Semidiscretized and Fully Discretized Systems in Computational Methods for Transient Analysis, edited by T. Belytschko and T. J. R. Hughes, Elsevier, 1983.

15) H. J. Sutherland, On the Separation of Geometric and Viscoelastic Dispersion in Composite Materials, Inter. Jour. of Solids and Structures, Vol. 11, pp. 233-246, 1975.

16) Z. Celep and Z. P. Bazant, Spurious Reflection of Elastic Waves Due to Gradually Changing Finite Element Size, Inter. Jour. Num. Meth. Engin., Vol. 19, pp. 631-646, 1983.

17) D. R. Bland, Wave Theory and Applications, Oxford University Press, 1988.

18) G. B. Whitham, Linear and Nonlinear Waves, Wiley, 1974.

19) P. W. Randles, Unpublished notes on dispersion, 1991-1992.

20) W. Flugge, Viscoelasticity, second edition, Springer-Verlag, 1975.

21) K. M. Wu, Preliminary Modeling of Compressive Shock and Spallation in Thick Composite Materials, NRL Memorandum Report 6684, July 1990.

22) R. M. Jones, Mechanics of Composite Materials, McGraw-Hill, 1975.

23) D. J. Benson, Computational Methods in Lagrangian and Eulerian Hydrocodes, Computer Methods in Applied Mechanics and Engineering 99, pp. 235-394, 1992.

8. APPENDICES

8.1 Appendix A - Reduced 1D damage model implemented in WONDY

As mentioned in the Introduction, WONDY has been used extensively in our work to study 1D plane strain behavior. In this appendix, the details of the 1D continuum damage model which has been programmed into WONDY are given. This constitutive model stems from the 2D damage theory developed in [1-3], and also includes the nonlinear response of the material in compression. Typical material and damage parameters are given for graphite/peek composite plates [6].

In the one dimensional WONDY computer models, the 1 direction is thru-the-thickness of the composite plate, while the 2 direction is inplane (1D plane strain models). The constitutive equation is given as follows:

$$\sigma_{11} = C_{11}(V_1)\,\varepsilon_{11} \qquad \textit{in tension} \qquad (8.1a)$$

$$\sigma_{11} = K_1\varepsilon_{11} + K_2\varepsilon_{11}^2 + K_3\varepsilon_{11}^3 \qquad \textit{in compression} \qquad (8.1b)$$

where σ_{11} is the stress, ε_{11} is the strain, C_{11} is the material stiffness, V_1 is the damage thru the thickness (delamination) and the K's are constants interpolated from the data in [6]. Typical values used for the K's for graphite/peek composite plates are:

$$K_1 = C_{11}(0) = 11.7\ GPa$$

$$K_2 = 114.\ GPa \qquad (8.2)$$

$$K_3 = 684.\ GPa$$

The damage model based upon [1-3] is expressed as:

$$C_{11}(V_1) = \frac{(1-\nu_{23})\,E_{11}(V_1)}{(1-\nu_{23}-2\nu_{12}^2(V_1)\,(E_{22}/(E_{11}(V_1))))}$$

$$E_{11}(V_1) = (1-V_1^2)\,E_{11}^0 \qquad (8.3)$$

$$\nu_{12}(V_1) = (1-V_1^2)\,\nu_{12}^0$$

in which E_{11} and E_{22} are the engineering moduli, and ν_{12} and ν_{23} are the Poisson's ratios. The evolution of the damage V_1 is in the form [1-3]:

$$\frac{dV_1}{dt} = \left(\frac{d_1(V_1, t)}{\sigma_{G0}}\right)^{n_1} / (\eta_1 (1 - V_1^2))$$

$$d_1(V_1, t) = Max[0, \sigma_{11} - \sigma_G] \qquad (8.4)$$

$$\sigma_G = (1 - V_1^2)\,\sigma_{G0}$$

In eqs (8.4), t is the time in seconds and d_1, σ_{G0}, n_1, η_1, σ_G and σ_{G0} are defined in [1-3]. Typical values used in eqs. (8.3) and (8.4) for graphite/peek are:

$$E_{11}^0 = 13.45\ GPa$$

$$E_{22} = 69.\ GPa$$

$$\nu_{12}^0 = 0.04 \qquad (8.5)$$

$$\nu_{23} = 0.30$$

and for the damage threshold parameters

$$\sigma_{G0} = 70.\ MPa$$

$$n_1 = 2. \qquad (8.6)$$

$$\eta_1 = 4. \times 10^{-6}\,\text{sec}$$

8.2 Appendix B - Listing of the ABAQUS/EXPLICIT user written subroutine for 2D continuum damage.

```
      SUBROUTINE VUMAT(
C...Read only variables
     1 NBLOCK,NDIR,NSHR,NSTATEV,NFIELDV,NPROPS,LANNEAL,
     2 STEP_TIME,TOTAL_TIME,DT,CMNAME,PROPS,DENSITY,
     3 STRAIN_INC,REL_SPIN_INC,
     4 TEMP_OLD,STRETCH_OLD,FIELD_OLD,
     5 STRESS_OLD,STATE_OLD,ENER_INTERN_OLD,ENER_INELAS_OLD,
     6 TEMP_NEW,STRETCH_NEW,FIELD_NEW,
C...Write only modifiable variables
     7 STRESS_NEW,STATE_NEW,ENER_INTERN_NEW,ENER_INELAS_NEW)
C.....................................
      INCLUDE 'ABA_PARAMS.INC'
C.....................................
C...This rountine is the 2d continuum damage theory developed
C    by Nemes and Randles and in the PRONTO2D code -
C    Transversely Isotropic Damage Model. Note as in PRONTO2D
C    the 1,2,3 axes in ABAQUS are not the same as given in the
C    report and paper 1->2, 2->3, 3->1     (from paper to ABAQUS
C    and PRONTO).  Nomenclature very similar to what Nemes used
C    in PRONTO2D has been employed. C.T. DYKA 10/92
C$$$$$$$$$$$$$$$$$$$$$$$$$$$$$$$$$$$$$$$$$$$$$$$$$$$$$$$$$$$
C...The 7 state variables are stored as for element I:
C       applies for old and state variables
C           STATE_OLD(I,1)=V1 (Thru thickness damage)
C           STATE_OLD(I,2)=V2 (In plane damage)
C           STATE_OLD(I,3)=DOUT (Switch for the death option)
C...&&&&&&&&&&&&&&&&&&&&
C...NOTE: Not sure ABAQUS/EXPLICIT has regular DEATH OPTION!!!!
C    ABAQUS does not track the strains, only the increments, so
C     use the state variables to track the total strains - which
C     we need to determine when the ultimate strain has been
C     reached.
C           STATE_OLD(I,4)=total strain(I,1)
C           STATE_OLD(I,5)=total strain(I,2)
C           STATE_OLD(I,6)=total strain(I,3)
C           STATE_OLD(I,7)=total strain(I,4)
C$$$$$$$$$$$$$$$$$$$$$$$$$$$$$$$$$$$$$$$$$$$$$$$$$$$$$$$$$$$
C...All arrays dimensioned by (*) are not used in this subroutine.
      DIMENSION PROPS(NPROPS),DENSITY(NBLOCK),
     1 STRAIN_INC(NBLOCK,NDIR+NSHR),REL_SPIN_INC(*),
     2 TEMP_OLD(*),STRETCH_OLD(*),
     3 FIELD_OLD(*),
     4 STRESS_OLD(NBLOCK,NDIR+NSHR),STATE_OLD(NBLOCK,NSTATEV),
     5 ENER_INTERN_OLD(*),ENER_INELAS_OLD(*),
     6 TEMP_NEW(*),STRETCH_NEW(*),
     7 FIELD_NEW(*),
     8 STRESS_NEW(NBLOCK,NDIR+NSHR),STATE_NEW(NBLOCK,NSTATEV),
     9 ENER_INTERN_NEW(*),ENER_INELAS_NEW(*)
      CHARACTER*8 CMNAME
C###########################################################
C...  Material Properties
        E110 = PROPS(1)
        E220 = PROPS(2)
        RNU210 = PROPS(3)
        RNU130 = PROPS(4)
        G210   = PROPS(5)
        A1     = PROPS(6)
        A2     = PROPS(7)
```

```
          A3      = PROPS(8)
          A4      = PROPS(9)
          ETA1    = PROPS(10)
          EN1     = PROPS(11)
          ETA2    = PROPS(12)
          EN2     = PROPS(13)
          SIGG0   = PROPS(14)
          TAUG0   = PROPS(15)
          PHIG0   = PROPS(16)
          PHIG1   = PROPS(17)
          SIGG0B  = PROPS(18)
          TAUG0B  = PROPS(19)
          PHIG0B  = PROPS(20)
          PHIG1B  = PROPS(21)
          EULT    = PROPS(22)
        DO 100 I=1,NBLOCK
C... Continuum damage variable and DOUT to track death
C...    of an element
          V1      = STATE_OLD(I,1)
          V2      = STATE_OLD(I,2)
          DOUT    = STATE_OLD(I,3)
C...OPTION TO KILL AN ELEMENT WITHOUT THE DEATH OPTION
            IF(DOUT .GE. .98)V1=.98
            IF(DOUT .GE. .98)V2=.98
C.....................................
C... Stresses (abreviations)
          SIG1 = STRESS_OLD(I,1)
          SIG2 = STRESS_OLD(I,2)
          SIG3 = STRESS_OLD(I,3)
          SIG4 = STRESS_OLD(I,4)
C
C---- UPDATE ELASTIC PARAMETERS.  Note the 1,2,3 directions are switched
C       from the reference report and paper
        E22=E220*(1.-V1**2)
        E11=E110*(1.-A1*V2**2)
        G21=G210*(1.-V1**2)*(1.-A2*V2**2)
        RNU21=RNU210*(1.-V1**2)*(1.-A3*V2**2)
        RNU13=RNU130*(1-A4*V2**2)
        C22=(1.-RNU13)*E22/(1.-RNU13-2.*RNU21**2*E11/E22)
        C12=RNU21*E11/(1.-RNU13-2.*RNU21**2*E11/E22)
        C11=(1./(1.+RNU13))*(1.-RNU21**2*E11/E22)*E11/(1.-RNU13-2.*
      1     RNU21**2*E11/E22)
        C13=(1./(1.+RNU13))*(RNU13+RNU21**2*E11/E22)*E11/(1.-RNU13-2.*
      1     RNU21**2*E11/E22)
        C44=2.*G21
C
C----UPDATE STRAINS - Note we use the state variables
C
          STATE_NEW(I,4) = STATE_OLD(I,4) + STRAIN_INC(I,1)
          STATE_NEW(I,5) = STATE_OLD(I,5) + STRAIN_INC(I,2)
          STATE_NEW(I,6) = STATE_OLD(I,6) + STRAIN_INC(I,3)
          STATE_NEW(I,7) = STATE_OLD(I,7) + STRAIN_INC(I,4)
C...Determine the largest strain in each element -for the DEATH option.
c... Look at strain(1,1) and strain(3,3) components only
          STRC = MAX(STATE_NEW(I,4),STATE_NEW(I,6))
C---- COMPUTE V1
C
        IF(V1 .GE. .98)GO TO 20
```

```
        SIGG = SIG2
        TAU = SIG4
        SIGGG = SIGG0*(1.-V1**2)
        TAUG = TAUG0*(1.-V1**2)
        PHIG = PHIG0 - (PHIG0-PHIG1)*V1**2
        CALL DCALC (SIGGG,TAUG,PHIG,SIGG,TAU,V1,D1,N)
        IF(N.GT.0) GO TO 105
        IF (D1.LT.0.00001) GO TO 10
        V1D = ((D1/SIGG0)**EN1)/(ETA1*(1.-V1**2))
        V1 = V1 + V1D*DT
        IF(V1.GT.0.98)V1=.98
C
C---- COMPUTE V2 (also called VS)
C
   10   IF (V2.GE.0.98) GO TO 20
        SIGG = .5*(SIG1+SIG3)
        TAU = SQRT(SIG4**2+.25*(SIG1-SIG3**2)
        SIGGB = SIGG0B/(1.-V2**2)
        TAUB = TAUG0B/(1-V2**2)
        PHIB = PHIG0B - (PHIG0B-PHIG1B)*V2**2
        CALL DCALC(SIGGB,TAUB,PHIB,SIGG,TAU,V2,D2,N)
        IF(N.GT.0) GO TO 105
        IF(D2.LT.0.00001) GO TO 20
        V2D= (D2/SIGG0B)**EN2/ETA2
        V2 = V2 +V2D*DT
        IF (V2.GE.0.98)V2=.98
C...NEMES ALSO USED - I'LL INCLUDE V2 DAMAGE TO KILL ELEMENT
   20   IF(V1 .GE. .98 .OR. STRC .GT. EULT .OR V2 .GE. .98)DOUT=1.0
C...
C   20   IF(STRC.GT.EULT)DOUT=1.0
C
C---- UPDATE STRESSES
C
        STRESS_NEW(I,1)=C11*STATE_NEW(I,4)+C12*STATE_NEW(I,5)+
     1                  C13*STATE_NEW(,6)
        STRESS_NEW(I,2)=C22*STATE_NEW(I,5)+C12*(STATE_NEW(I,4)+
     1                  STATE_NEW(I,6))
        STRESS_NEW(I,3)=C12*STATE_NEW(I,5)+C13*STATE_NEW(I,4)+
     1                  C11*STATE_NEW(I,6)
        STRESS_NEW(I,4)=C44*STATE_NEW(I,7)
C...Update state variables - damage V1,V2 and DOUT (element death)
        STATE_NEW(I,1) = V1
        STATE_NEW(I,2) = V2
        STATE_NEW(I,3) = DOUT
  100 CONTINUE
C
      RETURN
  105 CONTINUE
C...STOP CALCULATIONS N IS OUT OF BOUNDS
      STOP
      END
      SUBROUTINE DCALC (SIGG,TAUG,PHIG,SIG,TAU,V,D,N)
C... THIS SUBROUTINE DOES THE THRESHOLD CALCULATIONS FOR V1 AND VS
C...   (V2) DAMAGE.  EACH CALL IS FOR ONE OR THE OTHER
      D=0.
      N=0
C     SIGG=SIGG0*(1.-V**2)
C     TAUG=TAUG0*(1.-V**2)
```

```
C       PHIG=PHIG0-(PHIG0-PHIG1)*V**2
        F0=(TAUG/PHIG)**2/SIGG
        F1=.5*(F0+SIGG)
        F2=.5*(F0-SIGG)
        F3=PHIG*F2
        IF((F1-SIG)/F2.GE.SQRT(1.+(TAU/F3)**2))RETURN
        C1=F2*(F1-SIG)/(F2**2+F3**2)
        C2=F3*TAU/(F2**2+F3**2)
        IF(C1.LT.0.) GO TO 10
        X=C2
     5  X1=C2+C1*X/SQRT(1.+X**2)
        N=N+1
        IF(N.GT.100) RETURN
        XDIFF=ABS(X1-X)
        X=X1
        IF(XDIFF.GT.0.0001)GO TO 5
        GO TO 20
    10  X=C2/(1.-C1)
    15  X2=(1.+X**2)**1.5
        X1=(C2+C1*X**3/X2)/(1.-C1/X2)
        N=N+1
        IF (N.GT.100)RETURN
        XDIFF=ABS(X1-X)
        X=X1
        IF (XDIFF.GT.0.0001) GO TO 15
    20  TAU0 = F3*X
        SIG0 =F1-F2*SQRT(1.+X**2)
        D=SQRT((SIG-SIG0)**2+(TAU-TAU0)**2)
        N=0
        RETURN
        END
```